

Global $U(1)_L$ Breaking in Neutrinophilic 2HDM: From LHC Signatures to X-Ray Line

Weijian Wang ^{a*} and Zhi-Long Han ^{b†}

^a *Department of Physics, North China Electric Power University, Baoding 071003, China*

^b *School of Physics, Nankai University, Tianjin 300071, China*

(Dated: October 4, 2016)

Lepton number violation plays an essential role in many scenarios of neutrino mass generation and also provides new clues to search new physics beyond the standard model. We consider the neutrinophilic two-Higgs-doublet model (ν -2HDM) where additional right-handed neutral fermions N_{Ri} and a complex singlet scalar σ are also involved. In scalar sector, the global $U(1)_L$ symmetry is spontaneous broken, leading to Nambu-Goldstone boson, the Majoron J , accompanied by the Majorana neutrino mass generation. We find that the massless Majoron will induce large invisible Higgs decay, and current experiments have already set constraints on relevant parameters. For the first time, we point out that the ν -2HDM with N_{Ri} can be distinguished from other seesaw by the same sign tri-lepton signature $3\ell^\pm 4j + \cancel{E}_T$. More interesting, for $\mathcal{O}(\text{keV})$ scale Majoron, it is a good candidate of decaying dark matter to interpret the 3.5 keV and 511 keV line excesses by two different parameter spaces.

* wjnwang96@aliyun.com

† hanzhilong@mail.nankai.edu.cn

I. INTRODUCTION

In standard model, the total lepton number is conserved at classical level, yet it is violated in many scenarios beyond the standard model. A widely discussed scenario of the lepton number violation (LNV) appears in the models for neutrino mass generation. To explain the no-zero but tiny neutrino mass, the dimension-5 effective operator $f(\Phi L)(\Phi L)/\Lambda$ [1] is introduced so that the smallness of neutrino mass is attributed to the seesaw mechanism[2–4] where lepton number is violated at a scale higher than electroweak scale.

The mechanism of LNV may play a key role in the dark side of our universe. The point is that the pseudo-Nambu-Goldstone boson(pNGB), the Majoron J , arises from the spontaneous breaking of global $U(1)_L$ symmetry[5] and picks light mass from quantum gravitational effect[6, 7]. In Ref.[8, 9], Majoron as a keV dark matter (DM) candidate has been studied where high LNV scale (typically $10^3 - 10^6$ TeV) is required to guarantee the small coupling of Majoron with neutrinos and eventually produce a satisfactory DM relic density. Moreover, at one loop level there exists a sub-leading decay of the Majoron to two photons from its coupling to charged fermions, leading to further constraints from x- and γ -ray experiments. On the other hand, for a TeV LNV scale, the coupling of Majorons to standard model Higgs boson could be large. As a result, the new invisible decay modes of Higgs boson to Majorons is open and provide an interesting route to probe new physics at LHC[10, 11]. The possibility of Majoron as WIMP DM has also been studied in Ref.[12, 13] where a soft $U(1)_L$ breaking term is added to generate the Majoron mass.

In this paper, we investigate the LNV effect in the context of neutrinophilic two-Higgs-doublet model (ν -2HDM) [14–17] where one scalar doublet Φ gives masses to standard model fermions, while the other scalar doublet Φ_ν with small vacuum expectation value (VEV) generates the Dirac neutrino mass term. In fermion sector, the neutral right-handed fermion singlets N_{Ri} are introduced to give a natural suppression for the light Majorana neutrino masses. Different from the conventional type-I seesaw model[2], lepton numbers of N_{Ri} are set to be zero instead of one. In scalar sector, in addition to the SM doublet scalar Φ , a doublet scalar Φ_ν with lepton number $L = 1$ and a singlet scalar σ with $L = 1/2$ are also required to produce the spontaneous LNV process. Hence the scheme we proposed can be called “122” seesaw model in comparison with the “123” seesaw model proposed in Ref.[8, 9] where the “3” denotes the triplet scalar Δ in type-II seesaw [3].

The scale of LNV is still unknown, hence both low scale and high scale scenarios are considered in this work. In former case, the new massive particles are naturally with electroweak (EW) scale, and thus contribute rich phenomenon at LHC. For instance, a distinct same sign tripleton $3\ell^\pm 4j + \cancel{E}_T$ signature arising from the associated production of neutrinophilic scalars is unique, and therefore making this model

quite distinguishable. While for the massless Majoron, it will contribute to invisible decays of Higgs. By choosing certain parameters, we find that a large branching ratio of invisible Higgs decay is possible to escape current experimental constraints. In the scenario with high LNV scale, we postulate the existence of $\mathcal{O}(\text{keV})$ - $\mathcal{O}(\text{MeV})$ Majoron particle, which serves as a late-decaying dark matter. We find that the Majoron can decay into two photons. Hence the current experimental results of X-ray background can set the emission line constraints on the relevant parameters. As already pointed out in Ref.[13], the 3.5keV x-ray line observed by XMM-Newton observatory[18] can be naturally explained by $J \rightarrow \gamma\gamma$. In addition, we further consider the 511 keV line from the galactic bulge observed by INTEGRAL experiment[19]. It is suggested that the 511 keV line can be originated from the annihilation of positronium[20–22] or radiative decaying of degenerate fermionic DM[23]. In our model, we suggest that the 511 keV emission line can be originated from the decay of Majoron into low energy electron-positron pairs $J \rightarrow e^+e^-$. Then the positrons dissipate their kinetic energy by collisions with baryon galactic gas and eventually form the positronium with electrons in the cosmic dust.[24].

The paper is organized as follows. In Sec.II, we introduce the model and describe the details of the symmetry breaking. Possible constraints from astrophysics, lepton flavor violation, and direct collider searches are considered in Sec.III. In Sec.IV A, we discuss the contribution of massless Majoron to invisible decays of Higgs. Collider signatures, especially the LNV signatures, are carried out in Sec.IV B. In Sec.IV C, we consider the Majoron as decaying dark matter and X-ray sources, where the 3.5keV and 511keV line excesses are also interpreted. The conclusions are summarised in Sec.V.

II. THE 122 MAJORON MODEL

A. The Model

In addition to SM particles, we introduce a singlet scalar σ , a neutrinophilic doublet scalar Φ_ν , and neutral right-handed fermions N_{Ri} . The representations of new particles are listed in Table. I, where the fields transform under not only SM gauge group but also global $U(1)_L$ group. The lepton number assignment in Table. I forbids the interaction $\bar{L}\tilde{\Phi}_\nu N_R$, so that only Φ_ν couples with N_R . The quark and charged lepton sector, on the other hand, are the same as the ones in SM. Thus the FCNCs do not appear at tree level. The relevant interactions are

$$\mathcal{L}_N = -y\bar{L}\tilde{\Phi}_\nu N_R + \frac{1}{2}\bar{N}_R^c m_N N_R + \text{h.c.} \quad (1)$$

Without loss of generality, we take the diagonal basis for charged leptons and N_R .

Field	Spin	$SU(3)_c$	$SU(2)_L$	$U(1)_Y$	$U(1)_L$
N_{Ri}	1/2	1	1	0	0
Φ_ν	0	1	2	1/2	1
σ	0	1	1	0	1/2

TABLE I. New particles content under $G_{SM} \otimes U(1)_L$

The complete scalar potential is given by

$$V = -\mu_2^2 \Phi^\dagger \Phi + \mu_3^2 \Phi_\nu^\dagger \Phi_\nu + \lambda_1 (\Phi^\dagger \Phi)^2 + \lambda_2 (\Phi_\nu^\dagger \Phi_\nu)^2 + \lambda_3 (\Phi^\dagger \Phi)(\Phi_\nu^\dagger \Phi_\nu) + \lambda_4 (\Phi^\dagger \Phi_\nu)(\Phi_\nu^\dagger \Phi) - \mu_1^2 \sigma^\dagger \sigma + \beta_1 (\sigma^\dagger \sigma)^2 + \beta_2 (\Phi^\dagger \Phi)(\sigma^\dagger \sigma) + \beta_3 (\Phi_\nu^\dagger \Phi_\nu)(\sigma^\dagger \sigma) - k (\Phi^\dagger \Phi_\nu \sigma^2 + \text{h.c.}). \quad (2)$$

where after acquiring non-zero VEVs, the scalars are denoted as

$$\sigma = \frac{v_1 + R_1 + iI_1}{\sqrt{2}}, \quad \Phi = \begin{pmatrix} \phi^+ \\ \frac{v_2 + R_2 + iI_2}{\sqrt{2}} \end{pmatrix}, \quad \Phi_\nu = \begin{pmatrix} \phi_\nu^+ \\ \frac{v_3 + R_3 + iI_3}{\sqrt{2}} \end{pmatrix}. \quad (3)$$

The VEV of σ breaks the global symmetry $U(1)_L$ spontaneously through the last term in Eq. 2 and also accounts for the generation of Majorana neutrino masses. The minimization conditions are given by

$$\begin{aligned} \mu_1^2 &= \frac{-2\beta_1 v_1^3 - \beta_2 v_2^2 v_1 - \beta_3 v_3^2 v_1 + 2k v_1 v_2 v_3}{2v_1} \\ \mu_2^2 &= \frac{-2\lambda_1 v_2^3 - \lambda_3 v_3^2 v_2 - \lambda_4 v_2^2 v_3 - \beta_2 v_1^2 v_3 + k v_1^2 v_3}{2v_2} \\ \mu_3^2 &= \frac{-2\lambda_2 v_3^3 - \lambda_3 v_2^2 v_3 - \lambda_4 v_2^2 v_3 - \beta_3 v_1^2 v_3 + k v_1^2 v_2}{2v_3} \end{aligned} \quad (4)$$

Taking the parameter set $\mu_{1,2,3}^2 > 0$ and $k \ll 1$, one can derive the VEV of Φ_ν from Eq.(4) as following

$$v_3 \simeq \frac{k v_1^2 v_2}{2\mu_3^2 + \beta_3 v_1^2}. \quad (5)$$

One notes that for $\mu_3 \ll v_1$, we have

$$v_3 \simeq \frac{k}{\beta_3} v_2, \quad (6)$$

where v_3 is independent to the LNV scale v_1 . For $\mu_3 \gg v_1$, we have

$$v_3 \simeq k \frac{v_1^2}{\mu_3^2} v_2. \quad (7)$$

Since v_3 is tightly related to tiny neutrino masses, then one expects the VEV hierarchy $v_3 \ll v_2$ in the condition of smallness of k or $\mu_3 \gg v_1$. Notably, $k \Phi^\dagger \Phi_\nu \sigma^2$ term is the only source of $U(1)_L$ breaking, radiative corrections to k are proportional to k itself and are only logarithmically sensitive to the cutoff [16]. Thus, the VEV hierarchy $v_3 \ll v_2 \lesssim v_1$ is stable against radiative corrections [25].

B. Neutrino Masses and Mixing

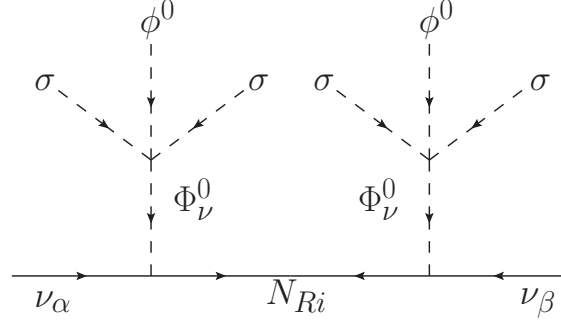


FIG. 1. The diagram for tree-level neutrino masses in our model.

Note that the term as $\lambda_5/2[(\Phi^\dagger\Phi_\nu)^2 + \text{h.c.}]$, which is allowed by discrete \mathbb{Z}_2 symmetry, is now forbidden by the global $U(1)_L$ symmetry in our model. As shown in Refs. [17, 26], such λ_5 term will contribute to one-loop induced neutrino masses, and the radiative induced neutrino masses would be dominant when $\lambda_5 v_2^2/(4\pi)^2 \gtrsim v_3^2$. Due to the forbiddance of such λ_5 term in our model, the neutrino masses are totally dominantly induced at tree-level as depicted in Fig. 1. Analogical to canonical Type-I seesaw [2], the mass matrix for light neutrinos can be written as

$$m_\nu = -\frac{v_3^2}{2} y m_N^{-1} y^T = U_{\text{PMNS}} \hat{m}_\nu U_{\text{PMNS}}^T, \quad (8)$$

where $\hat{m}_\nu = \text{diag}(m_1, m_2, m_3)$ is the diagonalized neutrino mass matrix, and U_{PMNS} is the PMNS (Pontecorvo-Maki-Nakagawa-Sakata) matrix:

$$U_{\text{PMNS}} = \begin{pmatrix} c_{12}c_{13} & s_{12}c_{13} & s_{13}e^{i\delta} \\ -s_{12}c_{23} - c_{12}s_{23}s_{13}e^{-i\delta} & c_{12}c_{23} - s_{12}s_{23}s_{13}e^{-i\delta} & s_{23}c_{13} \\ s_{12}s_{23} - c_{12}c_{23}s_{13}e^{-i\delta} & -c_{12}s_{23} - s_{12}c_{23}s_{13}e^{-i\delta} & c_{23}c_{13} \end{pmatrix} \times \begin{pmatrix} e^{i\varphi_1/2} & 0 & 0 \\ 0 & e^{i\varphi_2/2} & 0 \\ 0 & 0 & 1 \end{pmatrix} \quad (9)$$

Here, we use $c_{ij} = \cos \theta_{ij}$ and $s_{ij} = \sin \theta_{ij}$ for short, δ is the Dirac phase and φ_1, φ_2 are the two Majorana phases. In the following numerical discussion of the phenomenology, we take into account both normal (NH) and inverted hierarchy (IH), and use the latest best fit values of neutrino oscillation parameters in Ref. [27]¹. For simplicity, the Majorana phases $\varphi_{1,2}$ are neglected in the following numerical discussion. According to Eq. 8, the Yukawa matrix y can be expressed in terms of quantities measured in neutrino

¹ Early works on the global fit of neutrino oscillation can be found in Refs. [28].

oscillation experiments. Since the neutrino masses are induced by Type-I seesaw like mechanism in our model, we could adopt the Casas-Ibarra parametrization [29] to express y as:

$$y = \frac{\sqrt{2}}{v_3} U_{\text{PMNS}} \sqrt{\hat{m}_\nu} R \sqrt{m_N}, \quad (10)$$

where R is a complex orthogonal matrix. In the minimal case for two massive neutrinos, R can be expressed in terms of an angle ω [30] as:

$$R^{\text{NH}} = \begin{pmatrix} 0 & 0 \\ \sqrt{1-\omega^2} & -\omega \\ \omega & \sqrt{1-\omega^2} \end{pmatrix}, \quad R^{\text{IH}} = \begin{pmatrix} \sqrt{1-\omega^2} & -\omega \\ \omega & \sqrt{1-\omega^2} \\ 0 & 0 \end{pmatrix}, \quad (11)$$

for the normal (NH) and inverted (IH) hierarchy, respectively. Here in this work, we concentrate on the range $-1 < \omega < 1$. Typically, for $v_3 \sim 1\text{MeV}$, $m_\nu \sim 0.1\text{ eV}$ and $m_N \sim 100\text{ GeV}$, we have $y \sim 0.01$.

C. Scalar Masses and Mixings

The squared mass matrix for neutral CP-even scalars in the weak basis (R_1, R_2, R_3) is below

$$M_R^2 = \begin{pmatrix} 2\beta_1 v_1^2 & \beta_2 v_1 v_2 - k v_1 v_3 & \beta_3 v_1 v_3 - k v_1 v_2 \\ \beta_2 v_1 v_2 - k v_1 v_3 & 2\lambda_1 v_2^2 + \frac{1}{2} k v_1^2 \frac{v_3}{v_2} & (\lambda_3 + \lambda_4) v_2 v_3 - \frac{1}{2} k v_1^2 \\ \beta_3 v_1 v_3 - k v_1 v_2 & (\lambda_3 + \lambda_4) v_2 v_3 - \frac{1}{2} k v_1^2 & 2\lambda_2 v_3^2 + \frac{1}{2} k v_1^2 \frac{v_2}{v_3} \end{pmatrix}. \quad (12)$$

The M_R^2 is diagonalized by orthogonal matrix O^R as $O^R M_R^2 (O^R)^T = \text{diag}(m_{H_1}^2, m_{H_2}^2, m_{H_3}^2)$, where

$$\begin{pmatrix} H_1 \\ H_2 \\ H_3 \end{pmatrix} = O^R \begin{pmatrix} R_1 \\ R_2 \\ R_3 \end{pmatrix}, \quad (13)$$

and O^R is parameterized as

$$O^R = \begin{pmatrix} c_{12}c_{13} & c_{13}s_{12} & s_{13} \\ -s_{12}c_{23} - c_{12}s_{13}s_{23} & c_{12}c_{23} - s_{12}s_{13}s_{23} & c_{13}s_{23} \\ s_{23}s_{12} - c_{12}c_{23}s_{13} & -c_{12}s_{23} - c_{23}s_{12}s_{13} & c_{13}c_{23} \end{pmatrix}, \quad (14)$$

with $c_{ij} = \cos \alpha_{ij}$ and $s_{ij} = \sin \alpha_{ij}$ for short. In our following discussion, we will always keep H_2 to be the discovered standard model (SM) like Higgs boson with $m_{H_2} = 125\text{GeV}$ at LHC [31–33].

The squared mass matrix for CP-odd scalars in the basis (I_1, I_2, I_3) is given by

$$M_I^2 = k \begin{pmatrix} 2v_2 v_3 & -v_1 v_3 & v_1 v_2 \\ -v_1 v_3 & \frac{1}{2} v_1^2 \frac{v_3}{v_2} & -\frac{1}{2} v_1^2 \\ v_1 v_2 & -\frac{1}{2} v_1^2 & \frac{1}{2} v_1^2 \frac{v_2}{v_3} \end{pmatrix} \quad (15)$$

The matrix M_I^2 is diagonalized as $O^I M_I^2 (O^I)^T = \text{diag}(0, 0, m_A^2)$, where

$$\begin{pmatrix} J \\ G^0 \\ A \end{pmatrix} = O^I \begin{pmatrix} I_1 \\ I_2 \\ I_3 \end{pmatrix}. \quad (16)$$

As one could expect, two eigenstates with null masses are obtained, corresponding to the normal SM Goldstone boson G^0 and the Majoron J generated from global LNV. The m_A^2 and matrix O^I are given by

$$m_A^2 = k \left(\frac{v_1^2 v_3^2 + 4v_3^2 v_2^2 + v_1^2 v_2^2}{2v_2 v_3} \right), \quad (17)$$

$$O^I = \begin{pmatrix} cv_1 V^2 & 32cv_2 v_3^2 & -32cv_2^2 v_3 \\ 0 & -\frac{4v_2}{V} & -\frac{4v_3}{V} \\ -\frac{2bv_2}{v_1} & b & -\frac{bv_2}{v_3} \end{pmatrix}, \quad (18)$$

with

$$\begin{aligned} V^2 &= 16(v_2^2 + v_3^2) \\ c^{-2} &= v_1^2 V^4 + 1024(v_2^2 v_3^4 + v_2^4 v_3^2) \\ b^2 &= \frac{v_1^2 v_3^2}{v_2^2 v_1^2 + 4v_2^2 v_3^2 + v_3^2 v_1^2} \end{aligned} \quad (19)$$

Turning to the charged scalars, the associated squared mass matrix in the basis of (ϕ^\pm, ϕ_ν^\pm) is given by

$$M_{H^\pm}^2 = \frac{1}{2} \begin{pmatrix} kv_1^2 \frac{v_3}{v_2} - \lambda_4 v_3^2 & \lambda_4 v_2 v_3 - kv_1^2 \\ \lambda_4 v_2 v_3 - kv_1^2 & kv_1^2 \frac{v_2}{v_3} - \lambda_4 v_2^2 \end{pmatrix} \quad (20)$$

Then we have $O^\pm M_{H^\pm}^2 (O^\pm)^T = \text{diag}(0, m_{H^\pm}^2)$, where

$$\begin{pmatrix} G^\pm \\ H^\pm \end{pmatrix} = \begin{pmatrix} c_\pm & s_\pm \\ -s_\pm & c_\pm \end{pmatrix} \begin{pmatrix} \phi^\pm \\ \phi_\nu^\pm \end{pmatrix} \quad (21)$$

with $c_\pm = v_2 / \sqrt{v_2^2 + v_3^2}$, $s_\pm = v_3 / \sqrt{v_2^2 + v_3^2}$ and the mass of m_{H^\pm} given by

$$m_{H^\pm}^2 = \frac{1}{2v_2 v_3} (v_2^2 + v_3^2) (kv_1^2 - \lambda_4 v_2 v_3) \quad (22)$$

Taking into account the smallness of v_3 and k one notices from Eq.(12) that for the neutral scalars H_3 and A , the following mass relation holds approximately

$$m_A^2 \simeq kv_1^2 v_2 / 2v_3 = [M_R^2]_{33} \simeq m_{H_3}^2 \quad (23)$$

In the same way, from Eq.(17) and (22) one derives the mass relation

$$m_A^2 - m_{H^+}^2 \approx \frac{\lambda_4}{2} v_2^2, \quad (24)$$

which implies that the differences between m_A and m_{H^+} can not be too large under perturbativity condition. For simplicity, we will assume that masses of neutrinophilic scalars are degenerate, i.e., $m_{H^+} = m_{H^3} = m_A \equiv m_{\Phi_\nu}$.

III. CONSTRAINTS

A. Theoretical Constraints

Using Eqs.(12), (17) and (22), we rewrite all the coupling constants λ_i and β_j in terms of mixing angles α_{ij} and scalar masses

$$\begin{aligned} \beta_1 &= \frac{1}{2v_1^2} [M_R^2]_{11} \\ \beta_2 &= \frac{1}{v_1 v_2} [M_R^2]_{12} + k \frac{v_3}{v_1} \\ \beta_3 &= \frac{1}{v_1 v_3} [M_R^2]_{13} + k \frac{v_2}{v_3} \\ \lambda_1 &= \frac{1}{2v_2^2} [M_R^2]_{22} - k \frac{v_1^2 v_3}{4v_2^3} \\ \lambda_2 &= \frac{1}{2v_3^2} [M_R^2]_{33} - k \frac{v_1^2 v_2}{4v_3^3} \\ \lambda_3 &= \frac{1}{v_2 v_3} [M_R^2]_{23} - \lambda_4 + k \frac{v_1^2}{2v_2 v_3} \end{aligned} \quad (25)$$

and

$$\begin{aligned} \lambda_4 &= \frac{1}{v_2 v_3} (k v_1^2 - \frac{2v_2}{v_2 + v_3} m_{H^\pm}^2) \\ k &= \left(\frac{2v_2 v_3}{v_1^2 v_2^2 + v_3^2 v_2^2 + 4v_2^2 v_3^2} \right) m_A^2 \end{aligned} \quad (26)$$

where $[M_R^2]_{ij}$ denotes the matrix elements of M_R^2 .

The scalar potential is bounded from below if the quartic part of scalar potential is positive in the non-negative basis. In the following, we take the same procedure in Ref.[8, 9, 11]. Taking into account the fact of $v_3 \ll v_1$ and using Eq.(26), we derive the parameter k as

$$k \approx m_A^2 \frac{2v_3}{v_1^2 v_2} \quad (27)$$

Therefore, we have $k \ll \lambda_i, \beta_i$ and the parameter k can be neglected with respect to other coupling constants. In this limit, the *copositive* criteria[34] can be applied to the quartic part of scalar potential to give

the boundedness condition as following

$$\begin{aligned}
\lambda_1 &> 0, & \lambda_2 &> 0, & \beta_1 &> 0 \\
x &= \lambda_3 + \theta(-\lambda_4)\lambda_4 + 2\sqrt{\lambda_1\lambda_2} > 0 \\
y &= \beta_2 + 2\sqrt{\lambda_1\beta_1}, & z &= \beta_3 + 2\sqrt{\lambda_2\beta_1} \\
\sqrt{\lambda_1\lambda_2\beta_1} + [\lambda_3 + \theta(-\lambda_4)\lambda_4]\sqrt{\beta_1} + \beta_2\sqrt{\lambda_2} + \beta_3\sqrt{\lambda_1} + \sqrt{xyz} &> 0
\end{aligned} \tag{28}$$

In additional, we set the values of coupling constants λ_i and β_j less then $\sqrt{4\pi}$ to ensure the perturbative condition.

B. Astrophysical Constraints

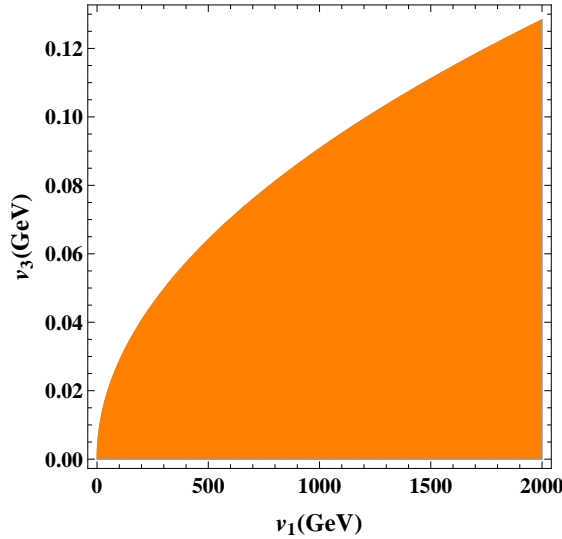


FIG. 2. Allowed region of v_3 as a function of v_1 considering the constraint from Majoron-electron coupling.

Note that $\rho = 1$ at tree level in this ν 2HDM. The stringent constraint on v_3 comes from astrophysics, due to the contributions of Majoron-electron coupling g_{Jee} to supernova [35] and red giant cooling [36]. For a massless Majoron (or lighter than typical stellar temperatures), the Compton-like process $\gamma + e \rightarrow J + e$ sets an upper bound for the g_{Jee} coupling as [35, 36]:

$$|g_{Jee}| = |O_{12}^I \frac{m_e}{v_2}| \lesssim 1.4 \times 10^{-13}. \tag{29}$$

Considering the profile of Majoron [37] in Eq. 46, we can translate this as a bound on the projection of the Majoron onto the doublet Φ as [38]:

$$|\langle J|\Phi \rangle| = \frac{2v_2v_3^2}{\sqrt{v_1^2(v_2^2 + v_3^2)^2 + 4v_2^2v_3^4 + 4v_2^4v_3^2}} \approx \frac{2v_3^2}{v_1v_2} \lesssim 6.7 \times 10^{-8}, \tag{30}$$

where in above approximation, we have used the assumption that $v_3 \ll v_1, v_2$. So from Eq. 30, we expect that $v_3^{\text{Max}} \propto \sqrt{v_1}$. The allowed region of v_3 as a function of v_1 is presented in FIG. 2. For instance, $v_3 \lesssim 0.09\text{GeV}$ must be satisfied when $v_1 = 1000\text{GeV}$.

C. Lepton Flavor Violation

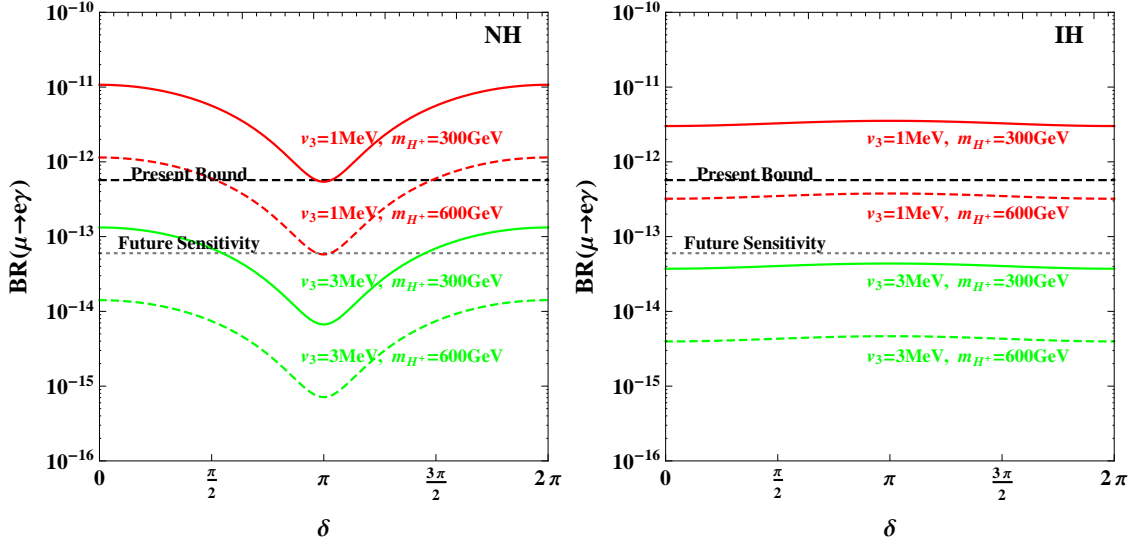


FIG. 3. $\text{BR}(\mu \rightarrow e\gamma)$ as a function of ω for four different values of v_3 and m_{H^+} in NH (left panel) and IH (right panel).

We find that the lepton flavor violating (LFV) processes would set a much more stringent lower bound on v_3 in models with heavy exotic leptons [39] than the canonical type-II seesaw [40, 41] as well as the Dirac neutrino scenario of $\nu 2\text{HDM}$ [42]. In this paper, we simply take the $\mu \rightarrow e\gamma$ process to illustrate such tight constraints, since the MEG experiment sets a severe upper limit as $\text{BR}(\mu \rightarrow e\gamma) < 5.7 \times 10^{-13}$ [43]. We also consider the future sensitivity of MEG experiment, which might be down to 6×10^{-14} [44]. The branching ratio of $\mu \rightarrow e\gamma$ is calculated as [45]:

$$\text{BR}(\mu \rightarrow e\gamma) = \frac{3\alpha}{64\pi G_F^2} \left| \sum_i \frac{y_{\mu i} y_{ei}^*}{m_{H^+}^2} F\left(\frac{m_{N_i}^2}{m_{H^+}^2}\right) \right|^2, \quad (31)$$

where the loop function $F(x)$ is:

$$F(x) = \frac{1 - 6x + 3x^2 + 2x^3 - 6x^2 \ln x}{6(1-x)^4}. \quad (32)$$

In Fig. 3, we show the numerical results of $\text{BR}(\mu \rightarrow e\gamma)$ as a function of ω for $(v_3, m_{H^+}) = (1\text{MeV}, 300\text{GeV})$, $(1\text{MeV}, 600\text{GeV})$, $(3\text{MeV}, 300\text{GeV})$ and $(3\text{MeV}, 600\text{GeV})$ in both normal and inverted hierarchy. In case of

normal hierarchy, the present MEG bound [43] requires $v_3 m_{H^+} \gtrsim 600 \text{MeV} \cdot \text{GeV}$, meanwhile the future MEG sensitivity [44] would push this bound up to $v_3 m_{H^+} \gtrsim 900 \text{MeV} \cdot \text{GeV}$. On the other hand in case of inverted hierarchy, the bound on $v_3 m_{H^+}$ is slightly less stringent than the the bound of normal hierarchy. Briefly, we can conclude that to satisfy the LFV constraint, $v_3 \gtrsim \mathcal{O}(\text{MeV})$ is needed for $m_{H^+} \sim \mathcal{O}(\text{TeV})$.

In general, LFV processes depends on neutrino masses, mixing angles, Dirac phase, as well as Majorana phases. In our assumption with degenerate N_R and real R matrix, we obtain

$$\begin{aligned} \sum_i y_{\mu i} y_{ei}^* \propto U_{PMNS} \hat{m}_\nu U_{PMNS}^\dagger = c_{12} c_{13} s_{12} c_{23} (m_{\nu_2} - m_{\nu_1}) \\ + c_{13} s_{13} s_{23} e^{-i\delta} [(m_3 - m_2) + c_{12}^2 (m_2 - m_1)] \end{aligned} \quad (33)$$

Therefore, the $\mu \rightarrow e\gamma$ sets no constraint on the Majorana phases and the R matrix. But for a large s_{13} , the branch ratio is sensitive to the Dirac phase δ .

Comparing to the bound on type-II seesaw $v_\Delta m_{H^{++}} \gtrsim 150 \text{eV} \cdot \text{GeV}$ [40]² and Dirac scenario of $\nu 2\text{HDM}$ $v_3 m_{H^+} \gtrsim 250 \text{eV} \cdot \text{GeV}$ [42], the bound on the Majorana scenario of $\nu 2\text{HDM}$ $v_3 m_{H^+} \gtrsim 600 \text{MeV} \cdot \text{GeV}$ is about 6 orders of magnitudes higher. Here we take Dirac and Majorana scenario of $\nu 2\text{HDM}$ to briefly estimate such great difference. From Eq. 31, it is clear that the constraint from LFV actually requires about the same order of the Yukawa coupling y , since the loop function $F(x)$ is of the same order in both Dirac and Majorana scenario if we also assume $m_N < m_{H^+}$. In Dirac scenario, $y^D \sim m_\nu / v_3^D$, while in Majorana scenario, $y^M \sim \sqrt{m_\nu m_N} / v_3^M$. For the same order of the Yukawa coupling, we could estimate that $v_3^M / v_3^D \sim \sqrt{m_N / m_\nu} \sim 10^6$ with $m_N \sim 10^2 \text{GeV}$ and $m_\nu \sim 0.1 \text{eV}$, which is just the result of the above discussion.

D. Collider Constraints

The status of the Higgs singlet H_1 has been extensively studied in Refs. [46–49]. We refer to Ref. [49] for a more detail and updated study on the constraints of H_1 . In the high mass region with $m_{H_1} > 130 \text{GeV}$, the allowed value for $\sin \alpha_{12}$ as a function of m_{H_1} is shown in FIG.1 of Ref. [49]. For example, $\sin \alpha_{12} \lesssim 0.3$ is required with $m_{H_1} = 300 \text{GeV}$. Although the invisible decay $H_1 \rightarrow JJ$ could affect the direct search bound to be less stringent, the indirect bound as from Higgs signal rate still requires $\sin \alpha_{12} < 0.36$ [49]. So we will consider $\sin \alpha_{12} = 0.3, 0.2, 0.1$ with $m_{H_1} = 300 \text{GeV}$ as our benchmark points for the high mass region in Sec. IV A.

However, in the low mass region with $m_{H_1} < 120 \text{GeV}$, the stringent bound in Ref. [49] is not applicable to our model. Mainly because the invisible decay $H_1 \rightarrow JJ$ is totally dominant in this region (see the detail

² v_Δ is the vacuum expectation value of Higgs triplet Δ , and $m_{H^{++}}$ is the mass of the doubly-charged scalar H^{++} in Δ .

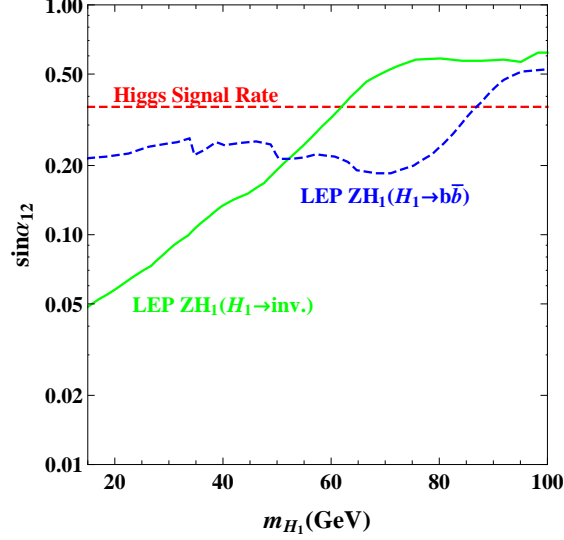


FIG. 4. Constraints on $\sin \alpha_{12}$ in the low mass region.

study in Sec. IV A). In FIG. 4, we show the constraints on $\sin \alpha_{12}$ in the low mass region coming from LHC Higgs signal rate [49], visible ($H_1 \rightarrow b\bar{b}$) [50] and invisible decaying ($H_1 \rightarrow JJ$) [51] Higgs at LEP through ZH_1 associated production. Note that for the constraint from $H_1 \rightarrow b\bar{b}$ we show the most severe case with $\text{BR}(H_1 \rightarrow b\bar{b}) = 1$. If we take into account a more realistic $\text{BR}(H_1 \rightarrow b\bar{b})$, the exclusion region will be $\sin \alpha_{12} > 0.4$ and less stringent than those from Higgs signal rate [10, 11]. For $m_{H_1} = 50\text{GeV}$, the most strict bound comes from invisible Higgs search at LEP with $\sin \alpha_{12} \lesssim 0.2$. Therefore, we will take $\sin \alpha_{12} = 0.2, 0.1, 0.05$ with $m_{H_1} = 50\text{GeV}$ as our benchmark points for the low mass region in Sec. IV A.

The collider signature of $\nu 2\text{HDM}$ has been discussed in Refs. [16, 17, 52]. In the case of $m_N > m_{H^+}$, the dominant decay mode of H^+ could be $H^+ \rightarrow \ell^+ \nu$. The direct search for signature as $\ell^+ \ell^- + \cancel{E}_T$ at LHC has excluded the region of $m_{H^+} \lesssim 300\text{GeV}$ [53, 54]. While in the case of $m_N < m_{H^+}$, the dominant decay mode of H^+ would be $H^+ \rightarrow \ell^+ N_{Ri}$ with the heavy Majorana neutrino N_{Ri} further decaying into $\ell^\pm W^\mp$, νZ and νH_2 . A detail discussion and simulation at LHC of this case is still missing. Therefor, we consider the LEP bound on charged scalar, i.e., $m_{H^+} > 80\text{GeV}$ [55]. And also to satisfy the constraints from electroweak precision tests (EWPT) [56], we further assume that the masses of neutrinophilic doublet scalars are degenerate as $m_{H^+} = m_{H_3} = m_A = m_{\Phi_\nu}$.

Since the heavy Majorana neutrino N_R also exists in canonical type-I seesaw [2], searches for N_R are already well studied [57–66]. For more detail, see the recent review of neutrino and collider in Ref. [67] and references therein. Direct searches for N_R at colliders have also been performed at LEP [68, 69] and LHC [70–72]. For $m_N < m_W$, LEP has excluded the mixing $V_{\ell N}$ between the heavy Majorana neutrino N and

the neutrino of flavor ν_ℓ with $|V_{\ell N}|^2 \gtrsim 2 \times 10^{-5}$ [68]. For a more heavier N_R , LHC would give the most restrictive direct limits. For instance, at $m_N = 200\text{GeV}$ the limit is $|V_{\ell N}|^2 < 0.017$ and at $m_N = 500\text{GeV}$ the limit is $|V_{\ell N}|^2 < 0.71$ [72]. In $\nu 2\text{HDM}$, the mixing $V_{\ell N}$ is predicted as [73]:

$$V_{\ell N} = U_{\text{PMNS}} \hat{m}_\nu^{1/2} R m_N^{-1/2} \sim 10^{-6} \quad (34)$$

for EW-scale m_N , which is far below current limits.

IV. PHENOMENOLOGY

As pointed in introduction, the LNV scale is still unknown, hence both low scale and high scale scenarios are allowed. For low scale scenario, our model is a natural TeV-model, so it can be test at LHC as we will discuss in SEC. IV A and IV B. On the other hand, if the Majoron are assumed to be a DM candidate, a high LNV scale $v_1 \gtrsim 10^4$ TeV are needed to satisfy constraints from WMAP. In high scale scenario, the natural way to get correct neutrino mass is keeping new scalar masses (i.e. m_{H^+} , m_{H_3} and m_A) around v_1 scale. So new scalars in case of massive Majoron are out reach of LHC. The possible signatures of massive Majoron will be discussed in SEC. IV C.

A. Invisible Higgs Decay

Due to the existence of massless Majoron J , the Higgs scalar can decay into Majorons though $H_a \rightarrow JJ$ and $H_a \rightarrow H_b H_b \rightarrow 4J$ [10, 11, 74, 75]. The Higgs-Majoron couplings are derived as:

$$g_{H_a JJ} = \left(\frac{(O_{11}^I)^2}{v_1} O_{1a}^R + \frac{(O_{12}^I)^2}{v_2} O_{2a}^R + \frac{(O_{13}^I)^2}{v_3} O_{3a}^R \right) m_{H_a}^2, \quad (35)$$

where O^R and O^I are the mixing matrices for CP-even and CP-odd scalars in Eq. 14 and 18. The partial decay width of $H_a \rightarrow JJ$ is then given by:

$$\Gamma(H_a \rightarrow JJ) = \frac{1}{32\pi} \frac{g_{H_a JJ}^2}{m_{H_a}}. \quad (36)$$

Similar to the type-II seesaw case [11], the smallness of v_3 indicates that the neutrinophilic doublet Φ_ν is basically decoupled. So we concentrate on the invisible decays of H_1 and H_2 . Note that for light $m_{H_3/A} < m_{H_2}/2$, H_3 or A could also mediate a sizable invisible decay of H_2 [76]. The trilinear coupling $H_2 H_1 H_1$ (see Eq. 55 in the appendix) contributes to invisible decay of SM Higgs H_2 with $H_1 \rightarrow JJ$. When $m_{H_1} < m_{H_2}/2$, the decay mode $H_2 \rightarrow H_1 H_1$ would be kinematically open. The partial decay width for $H_2 \rightarrow H_1 H_1$ is computed as:

$$\Gamma(H_2 \rightarrow H_1 H_1) = \frac{g_{H_2 H_1 H_1}^2}{32\pi m_{H_2}} \left(1 - \frac{4m_{H_1}^2}{m_{H_2}^2} \right)^{1/2}. \quad (37)$$

For the decays of H_1 into SM particles, we refer Ref. [46] for a more detail description. In this paper, the benchmark points discussed in Sec. IIID are used to illustrate the invisible decays of H_1 and H_2 . Varying the parameters, we find that the most relevant parameters for the invisible Higgs decays are $\sin \alpha_{12}$, v_1 , and m_{H_1} . For simplicity, we fix the value of the following parameters as:

$$\begin{aligned} m_{H^+} = m_{H_3} = m_A = m_{\Phi_\nu} &= 500 \text{ GeV}, \\ v_3 = 2 \text{ MeV}, \sin \alpha_{13} = \sin \alpha_{23} &= 2 \times 10^{-6}, \end{aligned} \quad (38)$$

meanwhile we vary the values of parameters $\sin \alpha_{12}$, v_1 , and m_{H_1} as:

$$\begin{aligned} \sin \alpha_{12} &\in [0, 0.3], \quad v_1 \in [500, 1500], \\ m_{H_1} &\in [10, 100] \text{ GeV, for the low mass region,} \\ &\in [200, 1000] \text{ GeV, for the high mass region.} \end{aligned} \quad (39)$$

It is checked that the above region is allowed by the boundedness conditions in Eq. 28. A fully scanning the whole parameter space as done in Refs. [10, 11] is worthwhile but beyond the scope of this paper. In the following, we will give some qualitative discussion which is helpful to better understand the scanning results of Refs. [10, 11].

1. High Mass Region:

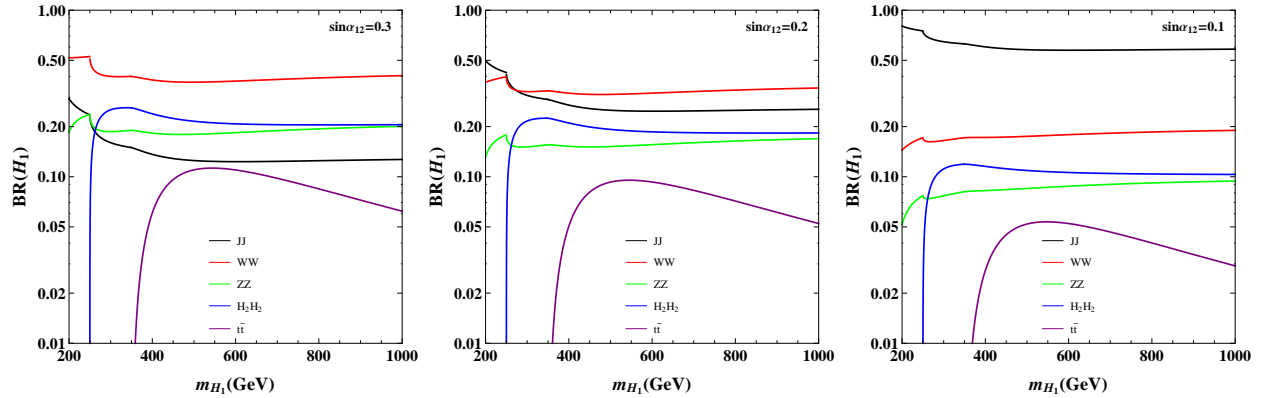


FIG. 5. Branching ratios of heavy singlet scalar H_1 as a function of m_{H_1} for $\sin \alpha_{12} = 0.3, 0.2, 0.1$, respectively. Here, we also set $v_1 = 1000 \text{ GeV}$.

First, we explore the high mass region $m_{H_1} > m_{H_2}$. In FIG. 5, we show the branching ratios of H_1 as a function of m_{H_1} for $\sin \alpha_{12} = 0.3, 0.2, 0.1$ with $v_1 = 1000 \text{ GeV}$. Clearly, the smaller $\sin \alpha_{12}$ is, the bigger $\text{BR}(H_1 \rightarrow JJ)$ is, thus the bigger invisible decay of H_1 is. For $\sin \alpha_{12} = 0.3$, $\text{BR}(H_1 \rightarrow JJ) \approx 0.14$ when $m_{H_1} > 350 \text{ GeV}$, which is smaller than $\text{BR}(H_1 \rightarrow W^+W^-, H_2H_2, ZZ)$. While for $\sin \alpha_{12} = 0.1$,

$\text{BR}(H_1 \rightarrow JJ) \approx 0.6$, which is the dominant decay channel and makes H_1 quite different from the real scalar singlet in Refs. [46–49]. If $m_{H_1} > 2m_{H_2}$, then $H_1 \rightarrow H_2 H_2 \rightarrow 4J$ will also contribute the invisible decay of H_1 , but $\text{BR}(H_1 \rightarrow 4J)$ is expected to be less than $0.3 \times 0.23^2 \approx 0.016$. On the other hand, $\text{BR}(H_1 \rightarrow JJ)$ is at least 0.14. Hence, the invisible decay of H_1 is dominant by $H_1 \rightarrow JJ$.

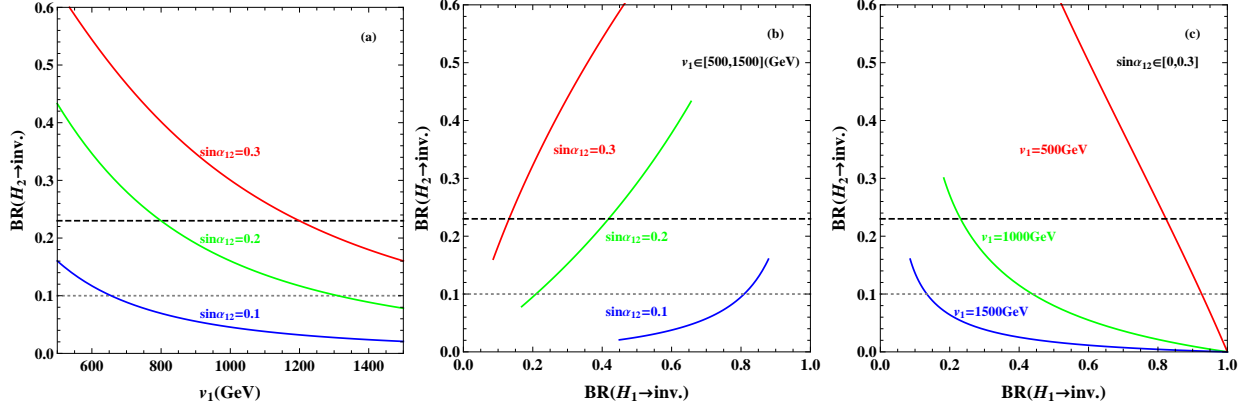


FIG. 6. (a) Branching ratios of invisible H_2 decay as a function of v_1 for $\sin \alpha_{12} = 0.3, 0.2, 0.1$. (b) Relations between $\text{BR}(H_1 \rightarrow \text{inv.})$ and $\text{BR}(H_2 \rightarrow \text{inv.})$ for $\sin \alpha_{12} = 0.3, 0.2, 0.1$ by varying v_1 in the range of 500–1500 GeV. (c) Relations between $\text{BR}(H_1 \rightarrow \text{inv.})$ and $\text{BR}(H_2 \rightarrow \text{inv.})$ for $v_1 = 500, 1000, 1500$ GeV by varying $\sin \alpha$ in the range of 0–0.3. In all these figures, we have set $m_{H_1} = 300$ GeV. The dashed and dotted line correspond to current (0.23) [77] and future limit (≈ 0.1) [78] on $\text{BR}(H_2 \rightarrow \text{inv.})$.

In the high mass region with $m_{H_1} > m_{H_2}$, the invisible H_2 decay is dominant by $H_2 \rightarrow JJ$. In FIG. 6 (a), we show $\text{BR}(H_2 \rightarrow \text{inv.})^3$ vs. v_1 for $\sin \alpha_{12} = 0.3, 0.2, 0.1$. It is obvious that a smaller $\sin \alpha_{12}$ (v_1) will lead to smaller (larger) $\text{BR}(H_2 \rightarrow \text{inv.})$ for fixed v_1 ($\sin \alpha_{12}$). Considering current bound on $\text{BR}(H_2 \rightarrow \text{inv.})$ [77], $v_1 \gtrsim 1200(800)$ GeV is required for $\sin \alpha_{12} = 0.3(0.2)$. We then show the relations between $\text{BR}(H_1 \rightarrow \text{inv.})$ and $\text{BR}(H_2 \rightarrow \text{inv.})$ with $m_{H_1} = 300$ GeV for $\sin \alpha_{12} = 0.3, 0.2, 0.1$ by varying v_1 in the range of 500–1500 GeV in FIG. 6 (b), and for $v_1 = 500, 1000, 1500$ GeV by varying $\sin \alpha$ in the range of 0–0.3 in FIG. 6 (c). From these figures, we expect a positive(negative) correlation between $\text{BR}(H_2 \rightarrow \text{inv.})$ and $\text{BR}(H_1 \rightarrow \text{inv.})$ for varying $v_1(\sin \alpha_{12})$.

2. Low Mass Region:

Then, we study the low mass region $m_{H_1} < m_{H_2}$. In FIG. 7, we depict the branching ratios of H_1 as a function of m_{H_1} for $\sin \alpha_{12} = 0.3, 0.2, 0.1$ with $v_1 = 1000$ GeV. Different from the high mass region, $H_1 \rightarrow JJ$ is totally dominant in the low mass region for all allowed values of $\sin \alpha_{12}$. We expect $\text{BR}(H_1 \rightarrow \text{inv.}) \gtrsim 0.9$. The dominant visible decay of H_1 is $H_1 \rightarrow b\bar{b}$, and $\text{BR}(H_1 \rightarrow b\bar{b})$ is typically

³ inv. is short for invisible.

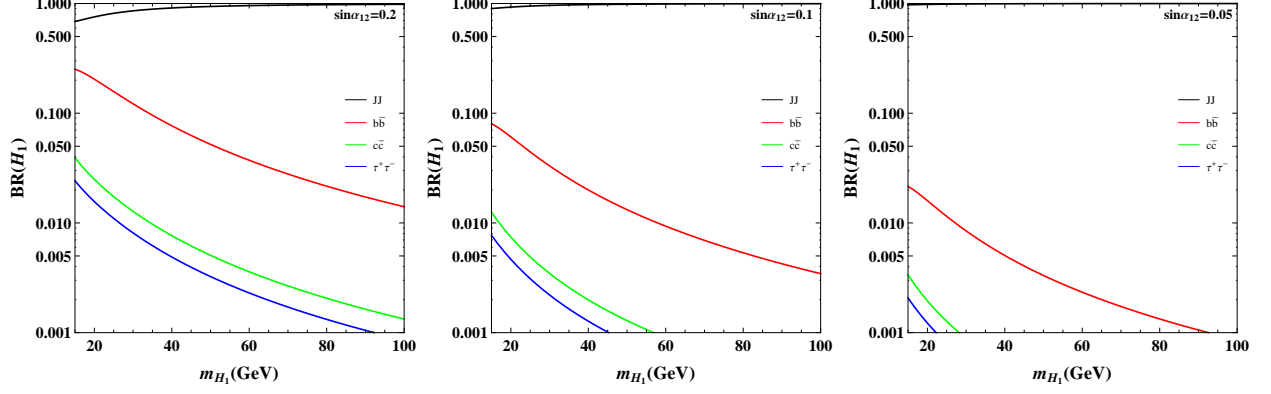


FIG. 7. Same as FIG. 5 but for $\sin \alpha_{12} = 0.2, 0.1, 0.05$ in the low mass region of m_{H_1} .

less than 0.1. So exotic H_2 decays as $H_2 \rightarrow H_1 H_1 \rightarrow b\bar{b} + \cancel{E}_T$ as well as $H_2 \rightarrow H_1 H_1 \rightarrow 4b$ would be challenging at LHC [79] for these benchmark points.

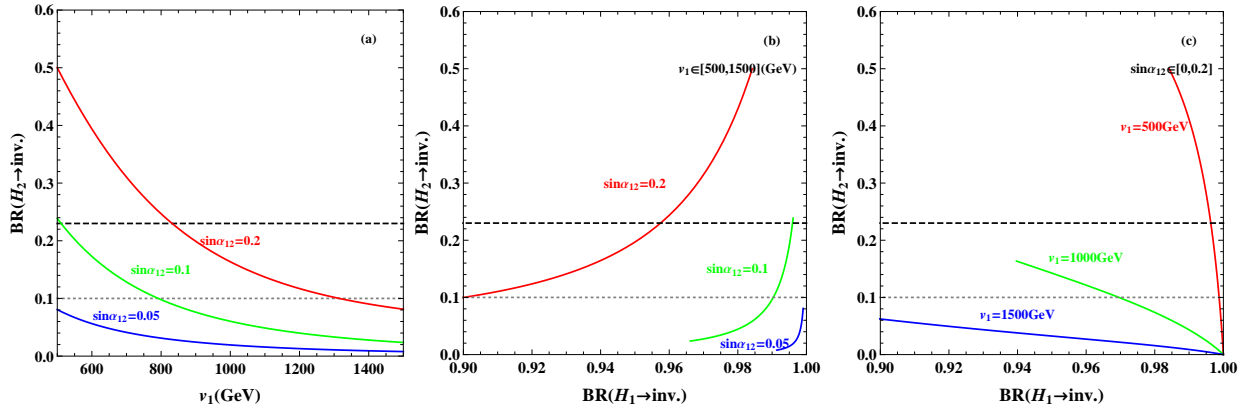


FIG. 8. Same as FIG. 6 but for $\sin \alpha_{12} = 0.2, 0.1, 0.05$ with $m_{H_1} = 50\text{GeV}$.

In the low mass region with $m_{H_1} < m_{H_2}/2$, $H_2 \rightarrow H_1 H_1 \rightarrow 4J$ will contribute to $H_2 \rightarrow \text{inv.}$. Fixed $m_{H_1} = 50\text{GeV}$, we present $\text{BR}(H_2 \rightarrow \text{inv.})$ vs. v_1 in FIG. 8 (a), $\text{BR}(H_2 \rightarrow \text{inv.})$ vs. $\text{BR}(H_1 \rightarrow \text{inv.})$ for $\sin \alpha_{12} = 0.2, 0.1, 0.05$ in FIG. 8 (b), and $\text{BR}(H_2 \rightarrow \text{inv.})$ vs. $\text{BR}(H_1 \rightarrow \text{inv.})$ for $v_1 = 500, 1000, 1500\text{GeV}$ in FIG. 8 (c). All the qualitative arguments in the high mass region are also applicable here. But due to contributions of $H_2 \rightarrow 4J$, bound on v_1 is slightly higher than it in the high mass case with same $\sin \alpha_{12}$. Since both $H_2 \rightarrow JJ$ and $H_2 \rightarrow 4J$ contribute to $H_2 \rightarrow \text{inv.}$, we quantize the contribution of $H_2 \rightarrow JJ$ to $H_2 \rightarrow \text{inv.}$ by defining:

$$R_{JJ} = \frac{\Gamma(H_2 \rightarrow JJ)}{\Gamma(H_2 \rightarrow \text{inv.})} = \frac{\Gamma(H_2 \rightarrow JJ)}{\Gamma(H_2 \rightarrow JJ) + \Gamma(H_2 \rightarrow 4J)}. \quad (40)$$

In FIG. 9, we plot the contour of R_{JJ} in the $\sin \alpha_{12}$ vs. v_1 plane. For $\sin \alpha_{12} > 0.01$, $R_{JJ} > 0.5$, which

indicates that $H_2 \rightarrow JJ$ is the dominant contribution to invisible H_2 decays in quite a large parameter space. And from FIG. 9, we could conclude that the larger v_1 or the smaller $\sin \alpha$ is, the smaller the contribution of $H_2 \rightarrow JJ$ to $H_2 \rightarrow \text{inv.}$ is.

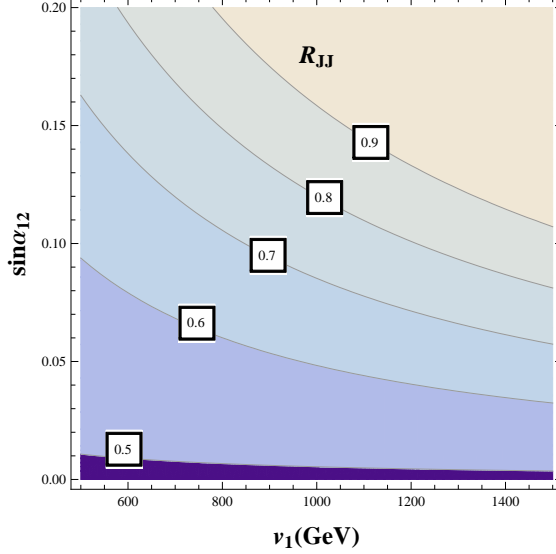


FIG. 9. Fraction of $H_2 \rightarrow JJ$ to total invisible H_2 decay with $m_{H_1} = 50\text{GeV}$ in the $\sin \alpha_{12}$ vs. v_1 plane.

B. Collider Signatures

Early papers on collider phenomenon of the $\nu 2\text{HDM}$ with heavy Majorana neutrino N_{Ri} can be found in Refs. [14, 17, 80], and they mainly concentrate on the charged scalar H^+ . Following Ref. [17], we give a brief discussion of the signatures at LHC by taking into account the contribution of neutral scalars H_3 and A in neutrinophilic 2HDM. In FIG. 10, we show the cross section of pair and associate production of the neutrinophilic doublet scalars at 14 TeV LHC. Typically for EW-scale m_{Φ_ν} , the cross sections are at the order of $\mathcal{O}(\text{fb})$. The cross section of associate production $H^\pm H_3/A$ is about twice larger than it of the pair production $H^+ H^-$ or $H_3 A$.

The decay properties of the neutrophilic doublet and the heavy Majorana neutrino are discussed in Ref. [17]. For $m_{\Phi_\nu} < m_N$, the dominant decay mode of H^+ is $H^+ \rightarrow \ell^+ \nu_i$ with $v_3 \lesssim \mathcal{O}(\text{MeV})$ due to the mixing between light and heavy neutrino. In this case, the most promising signatures at LHC is $H^+ H^- \rightarrow \ell^+ \ell^- + \cancel{E}_T$ [52]. On the other hand for $m_{\Phi_\nu} > m_N$, the dominant decay mode of H^+ is $H^+ \rightarrow \ell^+ N_{Ri}$ with $v_3 \lesssim \mathcal{O}(\text{GeV})$ [17]. The dominant decay mode of neutral scalars are reasonable to be $H_3 \rightarrow \nu_\ell N_{Ri}$ and $A \rightarrow \nu_\ell N_{Ri}$, since they have the same Yukawa coupling as H^+ . The heavy

Majorana neutrino N_{Ri} then decays as $N_{Ri} \rightarrow \ell^\pm W^\mp$, $N_{Ri} \rightarrow \nu_\ell Z$, $N_{Ri} \rightarrow \nu_\ell H_2$ [17, 60, 73, 81]⁴. For $m_N = 200\text{GeV}$, we have $\text{BR}(N_{Ri} \rightarrow \ell^\pm W^\mp) = 0.60$, $\text{BR}(N_{Ri} \rightarrow \nu_\ell Z) = 0.28$, and $\text{BR}(N_{Ri} \rightarrow \nu_\ell H_2) = 0.12$.

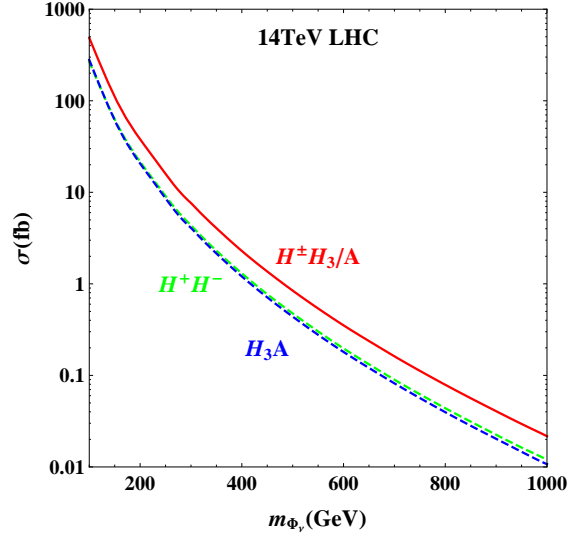


FIG. 10. Cross section of pair and associate production of the neutrophilic doublet scalars at 14 TeV LHC. We assume masses of the neutrophilic doublet scalars are degenerate as $m_{H^+} = m_{H_3} = m_A = m_{\Phi_\nu}$.

A : $H^+ H^- \rightarrow \ell^+ \ell^- N_{Ri} N_{Rj}$	B : $H^\pm H_3/A \rightarrow \ell^\pm \nu N_{Ri} N_{Rj}$	C : $H_3 A \rightarrow \nu \nu N_{Ri} N_{Rj}$
A.1: $\ell^+ \ell^- \ell^\pm W^\mp \ell^\pm W^\mp (0.360)$	B.1: $\ell^\pm \nu \ell^\pm W^\mp \ell^\pm W^\mp (0.360)$	C.1: $\nu \nu \ell^\pm W^\mp \ell^\pm W^\mp (0.360)$
A.2: $\ell^+ \ell^- \ell^\pm W^\mp \nu Z (0.336)$	B.2: $\ell^\pm \nu \ell^\pm W^\mp \nu Z (0.336)$	C.2: $\nu \nu \ell^\pm W^\mp \nu Z (0.336)$
A.3: $\ell^+ \ell^- \ell^\pm W^\mp \nu H_2 (0.144)$	B.3: $\ell^\pm \nu \ell^\pm W^\mp \nu H_2 (0.144)$	C.3: $\nu \nu \ell^\pm W^\mp \nu H_2 (0.144)$
A.4: $\ell^+ \ell^- \nu Z \nu Z (0.079)$	B.4: $\ell^\pm \nu \nu Z \nu Z (0.079)$	C.4: $\nu \nu \nu Z \nu Z (0.079)$
A.5: $\ell^+ \ell^- \nu Z \nu H_2 (0.067)$	B.5: $\ell^\pm \nu \nu Z \nu H_2 (0.067)$	C.5: $\nu \nu \nu Z \nu H_2 (0.067)$
A.6: $\ell^+ \ell^- \nu H_2 \nu H_2 (0.014)$	B.6: $\ell^\pm \nu \nu H_2 \nu H_2 (0.014)$	C.6: $\nu \nu \nu H_2 \nu H_2 (0.014)$

TABLE II. Signals from pair and associate production of neutrophilic doublet Φ_ν with their branching ratios given in the parentheses. Here, we set $m_N = 200\text{GeV}$.

In this paper, we concentrate on the case of $m_{\Phi_\nu} > m_N$. In TABLE II, we summarize all the possible signatures (in W^\pm, Z, H_2 level) and classify them into three collum according to the production mechanism of Φ_ν . With W^\pm, Z, H_2 further decaying, there are various possible signatures. Due to the existence of heavy Majorana neutrino N_{Ri} , we concentrate on LNV processes. The most interesting and distinct one is the same sign tri-lepton (SST) signature arising from B.1 of TABLE II :

$$\text{B.1} \rightarrow \ell^\pm \nu \ell^\pm jj \ell^\pm jj \rightarrow 3\ell^\pm 4j + \cancel{E}_T$$

⁴ For simplicity, we set all the mixing angles among scalars to be zero here.

To our knowledge, such SST signature with $\Delta L = 3$ can only take place in this model, thus it could be used to distinguish this model from other seesaw models. There are also several same sign di-lepton (SSD) signatures with $\Delta L = 2$:

$$\text{B.2} \rightarrow \ell^\pm \nu \ell^\pm jj \nu jj \rightarrow 2\ell^\pm 4j + \cancel{E}_T \quad (41)$$

$$\text{B.3} \rightarrow \ell^\pm \nu \ell^\pm jj \nu jj \rightarrow 2\ell^\pm 4j + \cancel{E}_T \quad (42)$$

$$\text{C.1} \rightarrow \nu \nu \ell^\pm jj \ell^\pm jj \rightarrow 2\ell^\pm 4j + \cancel{E}_T \quad (43)$$

All these three processes contribute to the SSD signature $2\ell^\pm 4j + \cancel{E}_T$. And there is also a four lepton signature with $\Delta L = 2$:

$$\text{A.1} \rightarrow \ell^+ \ell^- \ell^\pm jj \ell^\pm jj \rightarrow 3\ell^\pm \ell^\mp 4j \quad (44)$$

In FIG. 11, we shows the theoretical cross section for the LNV signatures at 14 TeV LHC. The SSD signature $2\ell^\pm 4j + \cancel{E}_T$ has the largest cross section, but it also suffers a relative large background from $t\bar{t}W$. On the contrary, the four lepton signature $3\ell^\pm \ell^\mp 4j$ has a relative clean background, but its cross section is the smallest. The SST signature $3\ell^\pm 4j + \cancel{E}_T$ seems very promising, since it is nearly background free. Thus it might be testable for $m_{\Phi_\nu} \lesssim 700\text{GeV}$ with integrated luminosity of 300fb^{-1} at 14 TeV LHC. A fully discussion and simulation of these LNV signatures at LHC will be carried out in another paper [82].

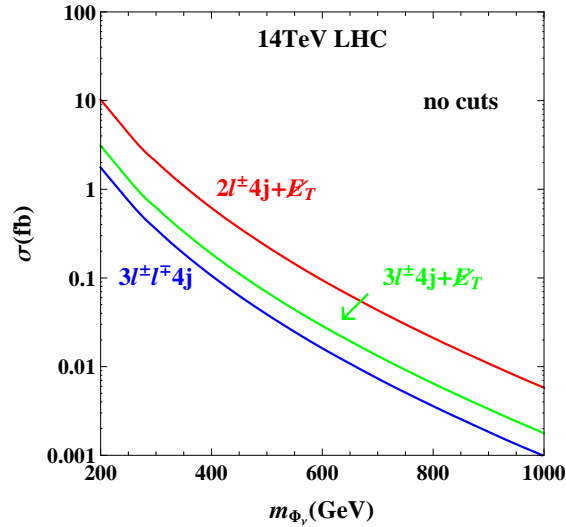


FIG. 11. Cross section of lepton number violation signatures at 14 TeV LHC. We also fix $m_N = 200\text{GeV}$.

C. Majoron Dark Matter

Considering the non-perturbative gravitational effects, the Majoron J could get an $\mathcal{O}(\text{keV})$ mass [6, 7], and play the role of decaying dark matter [8, 9, 83]. It is possible to realize EW-scale decaying [12, 13] or stable dark matter [84–86] in Majoron models. In this paper, we focus on $\mathcal{O}(\text{keV})$ Majoron and corresponding phenomenon.

For decaying Majoron dark matter, the present majoron density can be expressed as:

$$\Omega h^2 = \beta \left(\frac{m_J}{1.25 \text{ keV}} \right) e^{-t_0/\tau_J}, \quad (45)$$

where h is the Hubble constant, t_0 is the age of the universe, and β is in the range $10^{-5} - 1$ corresponding to the majoron thermal history [87]. The decay mode of Majoron J is dominant by $J \rightarrow \nu\nu$. Induced by the k -term in Eq. 2, the Majoron J has non-zero component along the SM and neutrinophilic doublet, and it is approximately given by:

$$J \sim I_1 + \frac{2v_3^2}{v_1 v_2} I_2 - \frac{2v_3}{v_1} I_3 \quad (46)$$

According to this, we can derive the Majoron-neutrino coupling (to leading order) [37]:

$$g_{J\nu_i\nu_j} = -\frac{2m_i^\nu}{v_1} \delta_{ij} + \dots \quad (47)$$

and the corresponding decay width:

$$\Gamma_{J \rightarrow \nu\nu} = \frac{m_J}{2\pi} \frac{\sum_i (m_i^\nu)^2}{v_1^2} \quad (48)$$

The late decay $J \rightarrow \nu\nu$ would produce too much power at large scales, thus spoiling the CMB anisotropy spectrum. WMAP third year data has set an upper limit [8, 88]:

$$\Gamma_J < 6.4 \times 10^{-19} s^{-1}, \text{ with } 0.12 \text{ keV} < \beta m_J < 0.17 \text{ keV}. \quad (49)$$

From Eq. 48, it is clear that such limit can be easily satisfied as long as v_1 is large enough. For instance, an $\mathcal{O}(\text{keV})$ Majoron requires $v_1 \gtrsim \mathcal{O}(10^4 \text{ TeV})$ to satisfy the WMAP limit. In the following discussion, we take v_1 to saturate the upper limit on $J \rightarrow \nu\nu$. Since $\beta \in [10^{-5}, 1]$, then $m_J \sim 0.1 - 10^4 \text{ keV}$. More interesting, the sub-leading decay mode of J is $J \rightarrow \gamma\gamma$, which is mediated by charged fermions at one-loop level:

$$\Gamma_{J \rightarrow \gamma\gamma} = \frac{\alpha^2 m_J^3}{64\pi^3} \left| \sum_f N_f Q_f^2 \frac{2v_3^2}{v_2^2 v_1} (-2T_3^f) \frac{m_J^2}{12m_f^2} \right|^2, \quad (50)$$

where N_f , Q_f , T_3^f and m_f are the color factor, electric charge, weak isospin and mass of SM fermion f , respectively. Note from Eq. 50 that, $\Gamma_{J \rightarrow \gamma\gamma}$ only depends on v_3 with fixed values of m_J and v_1 . The predicted decay rate of $J \rightarrow \gamma\gamma$ as a function of $E_\gamma (= m_J/2)$ for different values of v_3 is shown in FIG. 12. It is clear that a larger v_3 leads to a larger $\Gamma_{J \rightarrow \gamma\gamma}$. Since the performed line emission search has already excluded $\Gamma_{J \rightarrow \gamma\gamma} \gtrsim \mathcal{O}(10^{-28} s^{-1})$, a larger v_3 actually prefers a smaller E_γ for the survived γ -rays. Further considering the LFV bound on $v_3 \gtrsim \mathcal{O}(\text{MeV})$ with EW-scale m_{Φ_ν} , the predicted E_γ is usually $\lesssim 10 \text{ MeV}$, which covers the right region of m_J to satisfy the relic density of decaying dark matter [87].

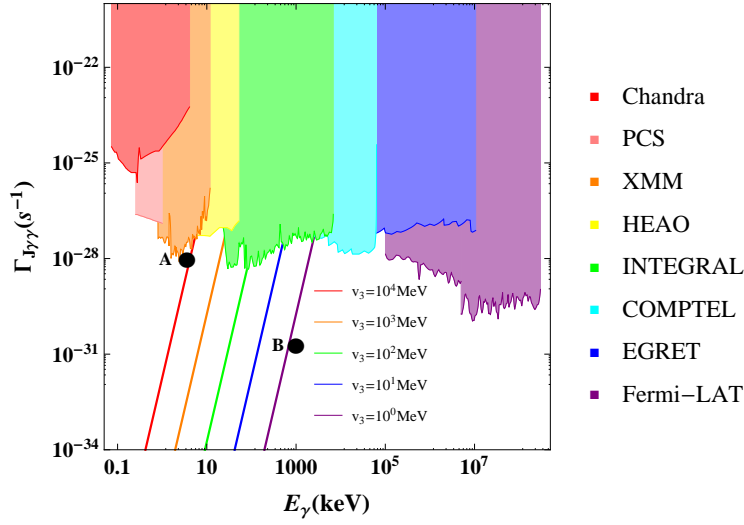


FIG. 12. The predicted decay rate of $J \rightarrow \gamma\gamma$ as a function of E_γ for different values of v_3 . Point A and B are the benchmark points to interpret the 3.5keV and 511keV line excess. The constraints are (from left to right): CHANDRA Low Energy Transmission Grating (LETG) observations of NGC3227 (red) [8], the Milky Way halo observed with PCS (pink) [89], XMM observations of the Milky Way and M31 (orange) [90], the diffuse x-ray background observed with HEAO (yellow) [91], INTEGRAL diffuse background (green)[92], COMPTEL search (cyan) [93], EGRET search (blue) [94], Fermi-LAT γ -ray searches (purple) [95].

As discussed in Sec. I, the Majoron DM is also a good candidate to explain several keV-line excesses. Here, we have chose two different benchmark points to interpret the observed 3.5 keV and 511 keV line excesses respectively. First, the direct decay mode $J \rightarrow \gamma\gamma$ for keV-scale Majoron can be used to interpret the 3.5 keV line excess with [13, 18]:

$$m_J \sim 7 \text{ keV}, \text{ and } \Gamma_{J \rightarrow \gamma\gamma} \sim 10^{-28} s^{-1}, \quad (51)$$

which corresponds to benchmark point A in FIG. 12. Such requirement can be satisfied with $v_3 \sim 10 \text{ GeV}$ and $v_1 \sim 10^4 \text{ TeV}$. Note that v_3 in this range can satisfy the tight astrophysical constraints for $v_1 \sim 10^4 \text{ TeV}$,

as well as the direct x-ray search bounds in FIG. 12 and WMAP limit in Eq. 49.

Second, for MeV-scale m_J , the decay mode $J \rightarrow e^+e^-$ is potential to explain the 511 keV line excess with the requirement [19–21]:

$$\Gamma_{J \rightarrow e^+e^-}^{\text{exp}} \simeq 6.3 \frac{m_J}{1\text{MeV}} \times 10^{-27} s^{-1}, \quad (52)$$

where we have assume that the Majoron DM J accounts for all the observed DM relic density. In our model, the decay width of $J \rightarrow e^+e^-$ is given by:

$$\Gamma_{J \rightarrow e^+e^-} = \frac{m_J}{8\pi} \left| \frac{2v_3^2}{v_1 v_2} \frac{m_e}{v_2} \right|^2 \left(1 - 4 \frac{m_e^2}{m_J^2} \right)^{1/2}. \quad (53)$$

Combine Eq. 52 and 53, we have:

$$\frac{\Gamma_{J \rightarrow e^+e^-}}{\Gamma_{J \rightarrow e^+e^-}^{\text{exp}}} = \left(\frac{v_3^2}{v_1 v_2} \right)^2 \left(1 - 4 \frac{m_e^2}{m_J^2} \right)^{1/2} \times 1.7 \times 10^{35}. \quad (54)$$

Taking $m_J = 2\text{MeV}$, the required decay width can be obtained for $v_3 \sim 1\text{MeV}$ and $v_1 \sim 10^6\text{TeV}$. Meanwhile the WMAP limit on Γ_J in Eq. 49 can be satisfied and the decay width of $\Gamma_{J \rightarrow \gamma\gamma}$ corresponding to benchmark point B in FIG. 12 is far below current direct x-ray limits. Note that to acquire $v_3 \sim 1\text{MeV}$, we also need $m_{\Phi_\nu} \gtrsim \text{TeV}$ to satisfy LFV constraints.

In principle, the discussions for invisible Higgs decay and LHC signatures in previous case for massless J are still applicable for Majoron DM, since J is still invisible at LHC and much lighter than electroweak scale. But with such large $v_1 \gtrsim 10^4 \text{ TeV}$ to satisfy WMAP limit, the coupling of $H_a J J$ is so small, thus the branching ratio of invisible Higgs decay is tiny. On the other hand, the masses of Φ_ν gets a large contribution from β_3 -term in the scalar potential and would be much heavier than TeV-scale, thus beyond the reach of LHC.

V. CONCLUSION

In this paper, we propose a new model to realize the spontaneous violation of global $U(1)_L$ symmetry in the context of ν -2HDM, where a neutrinophilic doublet scalar Φ_ν with lepton number $L = 1$, a complex singlet scalar σ with $L = 1/2$, and neutral right-handed fermion singlets N_{Ri} with $L = 0$ are introduced in addition to SM particles. The global $U(1)_L$ symmetry is spontaneously broken by the VEV of σ , which leads to an (nearly) massless Majoron J and also induces a small VEV of Φ_ν . Neutrino masses are generate at tree level type-I seesaw like diagram with the SM doublet Φ replaced by the neutrinophilic doublet Φ_ν . Due to the smallness of $\langle \Phi_\nu \rangle$, the model is naturally an $\mathcal{O}(\text{TeV})$ scale seesaw, and thus detectable in the reach of LHC.

Constraints coming from astrophysics, lepton flavor violation, and direct collider searches are taking into account. The astrophysical constraints set an upper limit on VEV of Φ_ν , i.e., $v_3 \lesssim 0.09\text{GeV}$ for the LNV scale v_1 at 1TeV. On the other hand, the LFV constraints set a lower limit on v_3 , i.e., $v_3 \gtrsim 1\text{MeV}$ for $m_{\Phi_\nu} = 600\text{GeV}$. Due to the existence of heavy N_R in Majorana case of ν -2HDM, we explain the huge enhancement ($\sim 10^6$) of lower limit on v_3 comparing to Dirac case of ν -2HDM. Based on various signals arising from new particles in our model, we investigate the direct search limits carried out by LEP and LHC as well. By choosing proper parameters, we find EW-scale new particles are allowed and some benchmark points are given to illustrate the phenomenological feature of the model.

For massless Majoron, two aspects of LHC signatures are studied: the invisible Higgs decays and LNV signatures. The invisible Higgs decays can be induced by $H_a \rightarrow JJ$ and $H_a \rightarrow H_b H_b \rightarrow 4J$. In the decoupling limit of Φ_ν , the two dominant variable that have impact on invisible Higgs decays are $\sin \alpha_{12}$ and v_1 . Comparing several benchmark points, we conclude that the Majoron could induce large invisible Higgs decay and future experiments prefer smaller $\sin \alpha_{12}$ and larger v_1 . The ν -2HDM with N_R has three kinds of LNV signatures. The most interesting and distinct one is the same sign tri-lepton signature $3\ell^\pm 4j + \cancel{E}_T$, which can be used to distinguish from other seesaw models. The other two LNV signatures $2\ell^\pm 4j + \cancel{E}_T$ and $3\ell^\pm \ell^\mp 4j$ are also promising to test this model at LHC.

Finally, the Majoron with $m_J \sim \mathcal{O}(\text{keV}) - \mathcal{O}(\text{MeV})$ mass is considered. In this case, the Majoron can serve as a good decaying dark matter candidate. To fulfill the CMB constraints on $\Gamma_{J \rightarrow \nu\nu}$, the LNV scale is required to be $\mathcal{O}(10^3 - 10^6\text{TeV})$. The sub-leading decay mode $J \rightarrow \gamma\gamma$ is also calculated and compared with current experiments. We find the current limits have already excluded some parameter space. Further, we point out that $J \rightarrow \gamma\gamma$ with $m_J \sim 7\text{keV}$ can explain the 3.5 keV line excess and $J \rightarrow e^+e^-$ with $m_J \sim \mathcal{O}(\text{MeV})$ can interpret the 511 keV line excess. Two different benchmark points are given to illustrate these two excesses respectively.

ACKNOWLEDGEMENT

The work of Weijian Wang is supported by National Natural Science Foundation of China under Grant Numbers 11505062, Special Fund of Theoretical Physics under Grant Numbers 11447117 and Fundamental Research Funds for the Central Universities.

APPENDIX

The coupling of $H_2 H_1 H_1$:

$$\begin{aligned}
\frac{g_{H_2 H_1 H_1}}{2} = & 3\lambda_1 v_2 (O_{12}^R)^2 O_{22}^R + 3\lambda_1 v_3 (O_{13}^R)^2 O_{23}^R + 3\beta_1 v_1 (O_{11}^R)^2 O_{21}^R \\
& + \frac{\lambda_3 + \lambda_4}{2} [(O_{13}^R)^2 O_{22}^R v_2 + (O_{12}^R)^2 O_{23}^R v_3 + 2O_{12}^R O_{13}^R (O_{23}^R v_2 + O_{22}^R v_3)] \\
& + \frac{\beta_2}{2} [(O_{12}^R)^2 O_{21}^R v_1 + (O_{11}^R)^2 O_{22}^R v_2 + 2O_{11}^R O_{12}^R (O_{22}^R v_1 + O_{21}^R v_2)] \\
& + \frac{\beta_3}{2} [(O_{13}^R)^2 O_{21}^R v_1 + (O_{11}^R)^2 O_{23}^R v_3 + 2O_{11}^R O_{13}^R (O_{23}^R v_1 + O_{21}^R v_3)] \\
& - \frac{k}{2} [(O_{11}^R)^2 O_{22}^R v_3 + (O_{11}^R)^2 O_{23}^R v_2 + 2O_{11}^R O_{12}^R (O_{21}^R v_3 + O_{23}^R v_1) + 2O_{11}^R O_{13}^R (O_{21}^R v_2 + O_{22}^R v_1)] .
\end{aligned} \tag{55}$$

-
- [1] S. Weinberg, Phys. Rev. Lett. **43**, 1566 (1979). doi:10.1103/PhysRevLett.43.1566
- [2] P. Minkowski, Phys. Lett. B **67**, 421 (1977), doi:10.1016/0370-2693(77)90435-X; T. Yanagida, in *Proceedings of the Workshop on Unified Theories and Baryon Number in the Universe*, eds. O. Sawada et al., (KEK Report 79-18, Tsukuba, 1979), p. 95; M. Gell-Mann, P. Ramond, R. Slansky, in *Supergravity*, eds. P. Van Nieuwenhuizen et al., (North-Holland, 1979), p. 315; S. Glashow, in *Quarks and Leptons*, Cargèses, eds. M. Lévy et al., (Plenum, 1980), p. 707; R. N. Mohapatra and G. Senjanovic, Phys. Rev. Lett. **44**, 912 (1980). doi:10.1103/PhysRevLett.44.912
- [3] W. Konetschny and W. Kummer, Phys. Lett. B **70**, 433 (1977). doi:10.1016/0370-2693(77)90407-5; T. P. Cheng and L. F. Li, Phys. Rev. D **22**, 2860 (1980). doi:10.1103/PhysRevD.22.2860; J. Schechter and J. W. F. Valle, Phys. Rev. D **22**, 2227 (1980). doi:10.1103/PhysRevD.22.2227
- [4] R. Foot, H. Lew, X. G. He and G. C. Joshi, Z. Phys. C **44**, 441 (1989). doi:10.1007/BF01415558
- [5] Y. Chikashige, R. N. Mohapatra and R. D. Peccei, Phys. Lett. B **98**, 265 (1981). doi:10.1016/0370-2693(81)90011-3; G. B. Gelmini and M. Roncadelli, Phys. Lett. B **99**, 411 (1981). doi:10.1016/0370-2693(81)90559-1; C. S. Aulakh and R. N. Mohapatra, Phys. Lett. B **119**, 136 (1982). doi:10.1016/0370-2693(82)90262-3
- [6] S. R. Coleman, Nucl. Phys. B **310**, 643 (1988). doi:10.1016/0550-3213(88)90097-1
- [7] R. Kallosh, A. D. Linde, D. A. Linde and L. Susskind, Phys. Rev. D **52**, 912 (1995) doi:10.1103/PhysRevD.52.912 [hep-th/9502069].
- [8] F. Bazzocchi, M. Lattanzi, S. Rieme-Sørensen and J. W. F. Valle, JCAP **0808** (2008) 013 doi:10.1088/1475-7516/2008/08/013 [arXiv:0805.2372 [astro-ph]]. M. Lattanzi, S. Rieme-Sørensen, M. Tortola and J. W. F. Valle, Phys. Rev. D **88** (2013) no.6, 063528 doi:10.1103/PhysRevD.88.063528 [arXiv:1303.4685 [astro-ph.HE]].
- [9] J. N. Esteves, F. R. Joaquim, A. S. Joshipura, J. C. Romao, M. A. Tortola and J. W. F. Valle, Phys. Rev. D **82**, 073008 (2010) doi:10.1103/PhysRevD.82.073008 [arXiv:1007.0898 [hep-ph]].

- [10] C. Bonilla, J. W. F. Valle and J. C. Romão, Phys. Rev. D **91**, no. 11, 113015 (2015) doi:10.1103/PhysRevD.91.113015 [arXiv:1502.01649 [hep-ph]].
- [11] C. Bonilla, J. C. Romão and J. W. F. Valle, New J. Phys. **18**, no. 3, 033033 (2016) doi:10.1088/1367-2630/18/3/033033 [arXiv:1511.07351 [hep-ph]].
- [12] P. H. Gu, E. Ma and U. Sarkar, Phys. Lett. B **690**, 145 (2010) doi:10.1016/j.physletb.2010.05.012 [arXiv:1004.1919 [hep-ph]].
- [13] F. S. Queiroz and K. Sinha, Phys. Lett. B **735**, 69 (2014) doi:10.1016/j.physletb.2014.06.016 [arXiv:1404.1400 [hep-ph]].
- [14] E. Ma, Phys. Rev. Lett. **86**, 2502 (2001) doi:10.1103/PhysRevLett.86.2502 [hep-ph/0011121].
- [15] S. Gabriel and S. Nandi, Phys. Lett. B **655**, 141 (2007) doi:10.1016/j.physletb.2007.04.062 [hep-ph/0610253].
- [16] S. M. Davidson and H. E. Logan, Phys. Rev. D **80**, 095008 (2009) doi:10.1103/PhysRevD.80.095008 [arXiv:0906.3335 [hep-ph]].
- [17] N. Haba and K. Tsumura, JHEP **1106**, 068 (2011) doi:10.1007/JHEP06(2011)068 [arXiv:1105.1409 [hep-ph]].
- [18] E. Bulbul, M. Markevitch, A. Foster, R. K. Smith, M. Loewenstein and S. W. Randall, Astrophys. J. **789** (2014) 13 doi:10.1088/0004-637X/789/1/13 [arXiv:1402.2301 [astro-ph.CO]]. A. Boyarsky, O. Ruchayskiy, D. Iakubovskiy and J. Franse, Phys. Rev. Lett. **113** (2014) 251301 doi:10.1103/PhysRevLett.113.251301 [arXiv:1402.4119 [astro-ph.CO]].
- [19] J. Knodlseder *et al.*, Astron. Astrophys. **411**, L457 (2003) doi:10.1051/0004-6361:20031437 [astro-ph/0309442].
- [20] C. Picciotto and M. Pospelov, Phys. Lett. B **605**, 15 (2005) doi:10.1016/j.physletb.2004.11.025 [hep-ph/0402178].
- [21] D. Hooper and L. T. Wang, Phys. Rev. D **70**, 063506 (2004) doi:10.1103/PhysRevD.70.063506 [hep-ph/0402220].
- [22] S. Khalil and O. Seto, JCAP **0810**, 024 (2008) doi:10.1088/1475-7516/2008/10/024 [arXiv:0804.0336 [hep-ph]].
- [23] T. Nomura, H. Okada and Y. Orikasa, arXiv:1603.04631 [hep-ph].
- [24] C. Boehm, D. Hooper, J. Silk, M. Casse and J. Paul, Phys. Rev. Lett. **92**, 101301 (2004) doi:10.1103/PhysRevLett.92.101301 [astro-ph/0309686].
- [25] N. Haba and T. Horita, Phys. Lett. B **705**, 98 (2011) doi:10.1016/j.physletb.2011.09.103 [arXiv:1107.3203 [hep-ph]].
- [26] E. Ma, Phys. Rev. D **73**, 077301 (2006) doi:10.1103/PhysRevD.73.077301 [hep-ph/0601225].
- [27] M. C. Gonzalez-Garcia, M. Maltoni and T. Schwetz, JHEP **1411** (2014) 052 doi:10.1007/JHEP11(2014)052 [arXiv:1409.5439 [hep-ph]].
- [28] D. V. Forero, M. Tortola and J. W. F. Valle, Phys. Rev. D **86** (2012) 073012 doi:10.1103/PhysRevD.86.073012 [arXiv:1205.4018 [hep-ph]]. G. L. Fogli, E. Lisi, A. Marrone, D. Montanino, A. Palazzo and A. M. Rotunno, Phys. Rev. D **86** (2012) 013012 doi:10.1103/PhysRevD.86.013012 [arXiv:1205.5254 [hep-ph]]. M. C. Gonzalez-Garcia, M. Maltoni, J. Salvado and T. Schwetz, JHEP **1212** (2012) 123 doi:10.1007/JHEP12(2012)123 [arXiv:1209.3023 [hep-ph]]. D. V. Forero, M. Tortola and J. W. F. Valle, Phys.

- Rev. D **90** (2014) no.9, 093006 doi:10.1103/PhysRevD.90.093006 [arXiv:1405.7540 [hep-ph]].
- [29] J. A. Casas and A. Ibarra, Nucl. Phys. B **618**, 171 (2001) doi:10.1016/S0550-3213(01)00475-8 [hep-ph/0103065].
 - [30] A. Ibarra and G. G. Ross, Phys. Lett. B **591**, 285 (2004) doi:10.1016/j.physletb.2004.04.037 [hep-ph/0312138].
 - [31] G. Aad *et al.* [ATLAS Collaboration], Phys. Lett. B **716**, 1 (2012) doi:10.1016/j.physletb.2012.08.020 [arXiv:1207.7214 [hep-ex]].
 - [32] S. Chatrchyan *et al.* [CMS Collaboration], Phys. Lett. B **716**, 30 (2012) doi:10.1016/j.physletb.2012.08.021 [arXiv:1207.7235 [hep-ex]].
 - [33] G. Aad *et al.* [ATLAS and CMS Collaborations], Phys. Rev. Lett. **114**, 191803 (2015) doi:10.1103/PhysRevLett.114.191803 [arXiv:1503.07589 [hep-ex]].
 - [34] K. Kannike, Eur. Phys. J. C **72**, 2093 (2012).
 - [35] D. S. P. Dearborn, D. N. Schramm and G. Steigman, Phys. Rev. Lett. **56**, 26 (1986). doi:10.1103/PhysRevLett.56.26
 - [36] N. Viaux, M. Catelan, P. B. Stetson, G. Raffelt, J. Redondo, A. A. R. Valcarce and A. Weiss, Phys. Rev. Lett. **111**, 231301 (2013) doi:10.1103/PhysRevLett.111.231301 [arXiv:1311.1669 [astro-ph.SR]].
 - [37] J. Schechter and J. W. F. Valle, Phys. Rev. D **25**, 774 (1982). doi:10.1103/PhysRevD.25.774
 - [38] M. A. Diaz, M. A. Garcia-Jareno, D. A. Restrepo and J. W. F. Valle, Nucl. Phys. B **527**, 44 (1998) doi:10.1016/S0550-3213(98)00434-9 [hep-ph/9803362].
 - [39] R. Ding, Z. L. Han, Y. Liao, H. J. Liu and J. Y. Liu, Phys. Rev. D **89**, no. 11, 115024 (2014) doi:10.1103/PhysRevD.89.115024 [arXiv:1403.2040 [hep-ph]].
 - [40] T. Fukuyama, H. Sugiyama and K. Tsumura, JHEP **1003**, 044 (2010) doi:10.1007/JHEP03(2010)044 [arXiv:0909.4943 [hep-ph]].
 - [41] Z. L. Han, R. Ding and Y. Liao, Phys. Rev. D **91**, 093006 (2015) doi:10.1103/PhysRevD.91.093006 [arXiv:1502.05242 [hep-ph]]. Z. L. Han, R. Ding and Y. Liao, Phys. Rev. D **92**, no. 3, 033014 (2015) doi:10.1103/PhysRevD.92.033014 [arXiv:1506.08996 [hep-ph]].
 - [42] E. Bertuzzo, Y. F. Perez G., O. Sumensari and R. Zukanovich Funchal, JHEP **1601**, 018 (2016) doi:10.1007/JHEP01(2016)018 [arXiv:1510.04284 [hep-ph]].
 - [43] J. Adam *et al.* [MEG Collaboration], Phys. Rev. Lett. **110**, 201801 (2013) doi:10.1103/PhysRevLett.110.201801 [arXiv:1303.0754 [hep-ex]].
 - [44] A. M. Baldini *et al.*, arXiv:1301.7225 [physics.ins-det].
 - [45] E. Ma and M. Raidal, Phys. Rev. Lett. **87**, 011802 (2001) Erratum: [Phys. Rev. Lett. **87**, 159901 (2001)] doi:10.1103/PhysRevLett.87.159901, 10.1103/PhysRevLett.87.011802 [hep-ph/0102255].
 - [46] T. Robens and T. Stefaniak, Eur. Phys. J. C **75**, 104 (2015) doi:10.1140/epjc/s10052-015-3323-y [arXiv:1501.02234 [hep-ph]].
 - [47] D. Buttazzo, F. Sala and A. Tesi, JHEP **1511**, 158 (2015) doi:10.1007/JHEP11(2015)158 [arXiv:1505.05488 [hep-ph]].

- [48] W. Wang and Z. L. Han, Phys. Rev. D **92**, 095001 (2015) doi:10.1103/PhysRevD.92.095001 [arXiv:1508.00706 [hep-ph]].
- [49] T. Robens and T. Stefaniak, arXiv:1601.07880 [hep-ph].
- [50] J. Abdallah *et al.* [DELPHI Collaboration], Eur. Phys. J. C **38**, 1 (2004) doi:10.1140/epjc/s2004-02011-4 [hep-ex/0410017].
- [51] G. Abbiendi *et al.* [OPAL Collaboration], Phys. Lett. B **682**, 381 (2010) doi:10.1016/j.physletb.2009.09.010 [arXiv:0707.0373 [hep-ex]].
- [52] S. M. Davidson and H. E. Logan, Phys. Rev. D **82**, 115031 (2010) doi:10.1103/PhysRevD.82.115031 [arXiv:1009.4413 [hep-ph]].
- [53] G. Aad *et al.* [ATLAS Collaboration], JHEP **1405**, 071 (2014) doi:10.1007/JHEP05(2014)071 [arXiv:1403.5294 [hep-ex]].
- [54] V. Khachatryan *et al.* [CMS Collaboration], Eur. Phys. J. C **74**, no. 9, 3036 (2014) doi:10.1140/epjc/s10052-014-3036-7 [arXiv:1405.7570 [hep-ex]].
- [55] G. Abbiendi *et al.* [ALEPH and DELPHI and L3 and OPAL and LEP Collaborations], Eur. Phys. J. C **73**, 2463 (2013) doi:10.1140/epjc/s10052-013-2463-1 [arXiv:1301.6065 [hep-ex]].
- [56] P. A. N. Machado, Y. F. Perez, O. Sumensari, Z. Tabrizi and R. Z. Funchal, JHEP **1512**, 160 (2015) doi:10.1007/JHEP12(2015)160 [arXiv:1507.07550 [hep-ph]].
- [57] W. Y. Keung and G. Senjanovic, Phys. Rev. Lett. **50**, 1427 (1983). doi:10.1103/PhysRevLett.50.1427
- [58] T. Han and B. Zhang, Phys. Rev. Lett. **97**, 171804 (2006) doi:10.1103/PhysRevLett.97.171804 [hep-ph/0604064].
- [59] F. del Aguila and J. A. Aguilar-Saavedra, Nucl. Phys. B **813**, 22 (2009) doi:10.1016/j.nuclphysb.2008.12.029 [arXiv:0808.2468 [hep-ph]].
- [60] A. Atre, T. Han, S. Pascoli and B. Zhang, JHEP **0905**, 030 (2009) doi:10.1088/1126-6708/2009/05/030 [arXiv:0901.3589 [hep-ph]].
- [61] P. S. B. Dev, A. Pilaftsis and U. k. Yang, Phys. Rev. Lett. **112**, no. 8, 081801 (2014) doi:10.1103/PhysRevLett.112.081801 [arXiv:1308.2209 [hep-ph]].
- [62] A. Das, P. S. Bhupal Dev and N. Okada, Phys. Lett. B **735** (2014) 364 doi:10.1016/j.physletb.2014.06.058 [arXiv:1405.0177 [hep-ph]].
- [63] D. Alva, T. Han and R. Ruiz, JHEP **1502**, 072 (2015) doi:10.1007/JHEP02(2015)072 [arXiv:1411.7305 [hep-ph]].
- [64] A. Das and N. Okada, Phys. Rev. D **88**, 113001 (2013) doi:10.1103/PhysRevD.88.113001 [arXiv:1207.3734 [hep-ph]].
- [65] S. Banerjee, P. S. B. Dev, A. Ibarra, T. Mandal and M. Mitra, Phys. Rev. D **92**, 075002 (2015) doi:10.1103/PhysRevD.92.075002 [arXiv:1503.05491 [hep-ph]].
- [66] A. Das, P. Konar and S. Majhi, arXiv:1604.00608 [hep-ph].
- [67] F. F. Deppisch, P. S. Bhupal Dev and A. Pilaftsis, New J. Phys. **17**, no. 7, 075019 (2015) doi:10.1088/1367-2630/17/7/075019 [arXiv:1502.06541 [hep-ph]].

- [68] P. Abreu *et al.* [DELPHI Collaboration], Z. Phys. C **74**, 57 (1997) Erratum: [Z. Phys. C **75**, 580 (1997)]. doi:10.1007/s002880050370
- [69] P. Achard *et al.* [L3 Collaboration], Phys. Lett. B **517**, 67 (2001) doi:10.1016/S0370-2693(01)00993-5 [hep-ex/0107014].
- [70] S. Chatrchyan *et al.* [CMS Collaboration], Phys. Lett. B **717**, 109 (2012) doi:10.1016/j.physletb.2012.09.012 [arXiv:1207.6079 [hep-ex]].
- [71] G. Aad *et al.* [ATLAS Collaboration], JHEP **1507**, 162 (2015) doi:10.1007/JHEP07(2015)162 [arXiv:1506.06020 [hep-ex]].
- [72] V. Khachatryan *et al.* [CMS Collaboration], arXiv:1603.02248 [hep-ex].
- [73] P. Fileviez Perez, T. Han and T. Li, Phys. Rev. D **80**, 073015 (2009) doi:10.1103/PhysRevD.80.073015 [arXiv:0907.4186 [hep-ph]].
- [74] A. S. Joshipura and S. D. Rindani, Phys. Rev. Lett. **69**, 3269 (1992). doi:10.1103/PhysRevLett.69.3269
- [75] A. S. Joshipura and J. W. F. Valle, Nucl. Phys. B **397**, 105 (1993). doi:10.1016/0550-3213(93)90337-O
- [76] O. Seto, Phys. Rev. D **92**, no. 7, 073005 (2015) doi:10.1103/PhysRevD.92.073005 [arXiv:1507.06779 [hep-ph]].
- [77] V. Khachatryan *et al.* [CMS Collaboration], Eur. Phys. J. C **75**, no. 5, 212 (2015) doi:10.1140/epjc/s10052-015-3351-7 [arXiv:1412.8662 [hep-ex]]. G. Aad *et al.* [ATLAS Collaboration], JHEP **1601**, 172 (2016) doi:10.1007/JHEP01(2016)172 [arXiv:1508.07869 [hep-ex]]. T. Corbett, O. J. P. Eboli, D. Goncalves, J. Gonzalez-Fraile, T. Plehn and M. Rauch, JHEP **1508**, 156 (2015) doi:10.1007/JHEP08(2015)156 [arXiv:1505.05516 [hep-ph]].
- [78] H. Okawa, J. Kunkle and E. Lipeles, arXiv:1309.7925 [hep-ex].
- [79] D. Curtin *et al.*, Phys. Rev. D **90**, no. 7, 075004 (2014) doi:10.1103/PhysRevD.90.075004 [arXiv:1312.4992 [hep-ph]].
- [80] S. Bar-Shalom, G. Eilam, T. Han and A. Soni, Phys. Rev. D **77**, 115019 (2008) doi:10.1103/PhysRevD.77.115019 [arXiv:0803.2835 [hep-ph]].
- [81] L. Basso, A. Belyaev, S. Moretti and C. H. Shepherd-Themistocleous, Phys. Rev. D **80**, 055030 (2009) doi:10.1103/PhysRevD.80.055030 [arXiv:0812.4313 [hep-ph]].
- [82] Z. L. Han, and Y. Liao, in preparing.
- [83] M. Lattanzi and J. W. F. Valle, Phys. Rev. Lett. **99**, 121301 (2007) doi:10.1103/PhysRevLett.99.121301 [arXiv:0705.2406 [astro-ph]].
- [84] M. Lindner, D. Schmidt and T. Schwetz, Phys. Lett. B **705**, 324 (2011) doi:10.1016/j.physletb.2011.10.022 [arXiv:1105.4626 [hep-ph]].
- [85] W. F. Chang and J. N. Ng, Phys. Rev. D **90**, no. 6, 065034 (2014) doi:10.1103/PhysRevD.90.065034 [arXiv:1406.4601 [hep-ph]].
- [86] W. F. Chang and J. N. Ng, arXiv:1604.02017 [hep-ph].
- [87] M. Frigerio, T. Hambye and E. Masso, Phys. Rev. X **1**, 021026 (2011) doi:10.1103/PhysRevX.1.021026 [arXiv:1107.4564 [hep-ph]].
- [88] M. Lattanzi, AIP Conf. Proc. **966**, 163 (2007) doi:10.1063/1.2836988 [arXiv:0802.3155 [astro-ph]].

- [89] A. Boyarsky, J. W. den Herder, A. Neronov and O. Ruchayskiy, *Astropart. Phys.* **28** (2007) 303 doi:10.1016/j.astropartphys.2007.06.003 [astro-ph/0612219].
- [90] A. Boyarsky, J. Nevalainen and O. Ruchayskiy, *Astron. Astrophys.* **471** (2007) 51 doi:10.1051/0004-6361:20066774 [astro-ph/0610961]. A. Boyarsky, D. Iakubovskiy, O. Ruchayskiy and V. Savchenko, *Mon. Not. Roy. Astron. Soc.* **387** (2008) 1361 doi:10.1111/j.1365-2966.2008.13266.x [arXiv:0709.2301 [astro-ph]].
- [91] A. Boyarsky, A. Neronov, O. Ruchayskiy and M. Shaposhnikov, *Mon. Not. Roy. Astron. Soc.* **370** (2006) 213 doi:10.1111/j.1365-2966.2006.10458.x [astro-ph/0512509]. A. Boyarsky, A. Neronov, O. Ruchayskiy, M. Shaposhnikov and I. Tkachev, *Phys. Rev. Lett.* **97** (2006) 261302 doi:10.1103/PhysRevLett.97.261302 [astro-ph/0603660].
- [92] A. Boyarsky, D. Malyshev, A. Neronov and O. Ruchayskiy, *Mon. Not. Roy. Astron. Soc.* **387** (2008) 1345 doi:10.1111/j.1365-2966.2008.13003.x [arXiv:0710.4922 [astro-ph]].
- [93] H. Yuksel and M. D. Kistler, *Phys. Rev. D* **78** (2008) 023502 doi:10.1103/PhysRevD.78.023502 [arXiv:0711.2906 [astro-ph]]. R. Essig, E. Kuflik, S. D. McDermott, T. Volansky and K. M. Zurek, *JHEP* **1311** (2013) 193 doi:10.1007/JHEP11(2013)193 [arXiv:1309.4091 [hep-ph]].
- [94] A. W. Strong, I. V. Moskalenko and O. Reimer, *Astrophys. J.* **613** (2004) 962 doi:10.1086/423193 [astro-ph/0406254].
- [95] M. Ackermann *et al.* [Fermi-LAT Collaboration], *Phys. Rev. D* **86** (2012) 022002 doi:10.1103/PhysRevD.86.022002 [arXiv:1205.2739 [astro-ph.HE]]. M. Ackermann *et al.* [Fermi-LAT Collaboration], *Phys. Rev. D* **88** (2013) 082002 doi:10.1103/PhysRevD.88.082002 [arXiv:1305.5597 [astro-ph.HE]]. A. Albert *et al.* [Fermi-LAT Collaboration], *JCAP* **1410** (2014) no.10, 023 doi:10.1088/1475-7516/2014/10/023 [arXiv:1406.3430 [astro-ph.HE]].